

1 **Impacts of future land use and land cover change on mid-21st-**
2 **century surface ozone air quality: Distinguishing between the**
3 **biogeophysical and biogeochemical effects**

4
5
6 Lang Wang^{1,2}, Amos P. K. Tai^{1,3,4}, Chi-Yung Tam^{1,3}, Mehliyar Sadiq^{1,3}, Peng Wang³,

7 Kevin K. W. Cheung⁵

8 1 Institute of Environment, Energy and Sustainability, The Chinese University of
9 Hong Kong, Hong Kong, China

10 2 Department of Geography and Resource Management, The Chinese University of
11 Hong Kong, Hong Kong, China

12 3 Earth System Science Programme, Faculty of Science, The Chinese University of
13 Hong Kong, Hong Kong, China

14 4 Partner State Key Laboratory of Agrobiotechnology, The Chinese University of
15 Hong Kong, Hong Kong, China

16 5 Department of Earth and Environmental Sciences, Macquarie University, Sydney,
17 Australia

18
19
20
21
22
23
24 Prepared for Atmospheric Chemistry and Physics

25 July 2020

26

Abstract

27 Surface ozone (O₃) is an important air pollutant and greenhouse gas. Land use
28 and land cover is one of the critical factors influencing ozone, in addition to
29 anthropogenic emissions and climate. Land use and land cover change (LULCC) can
30 on the one hand affect ozone “biogeochemically”, i.e., via dry deposition and
31 biogenic emissions of volatile organic compounds (VOCs). LULCC can on the other
32 hand alter regional- to large-scale climate through modifying albedo and
33 evapotranspiration, which can lead to changes in surface temperature,
34 hydrometeorology and atmospheric circulation that can ultimately impact ozone
35 “biogeophysically” over local and remote areas. Such biogeophysical effects of
36 LULCC on ozone are largely understudied. This study investigates the individual and
37 combined biogeophysical and biogeochemical effects of LULCC on ozone, and
38 explicitly examines the critical pathway for how LULCC impacts ozone pollution. A
39 global coupled atmosphere-chemistry-land model is driven by projected LULCC from
40 the present day (2000) to future (2050) under RCP4.5 and RCP8.5 scenarios, focusing
41 on the boreal summer. Results reveal that when considering biogeochemical effects
42 only, surface ozone is predicted to have slight changes by up to 2 ppbv maximum in
43 some areas due to LULCC. It is primarily driven by changes in isoprene emission and
44 dry deposition counteracting each other in shaping ozone. In contrast, when
45 considering the combined effect of LULCC, ozone is more substantially altered by up
46 to 5 ppbv over several regions in North America and Europe under RCP4.5, reflecting
47 the importance of biogeophysical effects on ozone changes. In boreal and temperate
48 mixed forests with intensive reforestation, enhanced net radiation and sensible heat
49 induce a cascade of hydrometeorological feedbacks that generate warmer and drier
50 conditions favorable for higher ozone levels. In contrast, reforestation in subtropical

51 broadleaf forests has minimal impacts on boundary-layer meteorology and ozone air
52 quality. Furthermore, significant ozone changes are also found in regions with only
53 modest LULCC, which can only be explained by “remote” biogeophysical effects. A
54 likely mechanism is that reforestation induces a circulation response, leading to
55 reduced moisture transport and ultimately warmer and drier conditions in the
56 surrounding regions with limited LULCC. We conclude that the biogeophysical
57 effects of LULCC are important pathways through which LULCC influences ozone
58 air quality both locally and in remote regions even without significant LULCC.
59 Overlooking the effects of hydrometeorological changes on ozone air quality may
60 cause underestimation of the impacts of LULCC on ozone pollution.

61

62 **Keywords:** ozone pollution; land use and land cover change; biogeochemical effects;
63 biogeophysical effects; hydrometeorology

64

65 **1. Introduction**

66 Surface ozone (O₃), as a harmful air pollutant, has negative consequences for
67 human health (WHO, 2005; Jerrett et al., 2009; Malley et al., 2017), decreases plant
68 gross primary productivity (e.g., Yue and Unger 2014), and leads to substantial
69 reductions in global crop yields (Avnery et al., 2011; Tai et al., 2014; Tian et al.,
70 2016; Tai and Val Martin, 2017; Mills et al., 2018). It is also an important greenhouse
71 gas, contributing to climate change (Myhre et al., 2013). Surface ozone is produced
72 by the photooxidation of precursors including carbon monoxide (CO), methane
73 (CH₄), and other non-methane volatile organic compounds (NMVOCs) in the
74 presence of nitrogen oxides (NO_x). These precursors are both generated by human
75 activities and naturally emitted from vegetation and soils. The dominant sink of
76 surface ozone is photochemical loss and dry deposition to the surface including
77 vegetation mainly in the form of leaf stomatal uptake. Depending on all of these
78 production and loss mechanisms, its concentration is highly sensitive to changes in
79 natural and anthropogenic emissions of precursors (Wang et al., 2011), land use and
80 land cover (Ganzeveld et al., 2010; Val Martin et al., 2015; Fu and Tai, 2015) and
81 climate (Jacob and Winner, 2009; Fiore et al., 2012; Schnell et al., 2016). Recent
82 studies found that decreases in anthropogenic emissions alone might not necessarily
83 decrease ozone in some polluted regions if factors such as climatic and land cover
84 changes act to enhance ozone and offset emission control efforts (Zhou et al., 2013;
85 Zhang et al., 2014; Xue et al., 2014).

86 Land use and land cover change (LULCC) can modify ozone concentration by
87 altering key drivers of ozone such as biogenic VOC emissions and dry deposition
88 (e.g., Wong et al., 2018). These can be referred to as “biogeochemical effects” of
89 LULCC on ozone (as opposed to “biogeophysical effects”, which will be discussed

90 next), because these processes entail directly modifying the biosphere-atmosphere
91 exchange of gases and particles that alters atmospheric composition including ozone
92 itself. Here we limit the “biogeochemical effects” of LULCC on ozone to processes
93 that influence ozone directly in a given climate, including biogenic VOC emission
94 and the dry deposition of ozone and its precursors; climatic changes that can arise
95 from land cover disturbances of the biogeochemical cycles are not the focus.

96 LULCC can modify the spatial pattern and magnitude of isoprene emission
97 due to their strong dependence on vegetation type and leaf density (Guenther et al.,
98 2012). For instance, Lathière et al. (2006) found as much as a 29% decrease in global
99 isoprene emission from a scenario in which 50% tropical trees are replaced by
100 grasses. Heald and Spracklen (2015) estimated the net effect of LULCC under future
101 anthropogenic influences as a decrease of 12–15% in annual isoprene emission
102 globally. These changes in isoprene emission can in turn modify ozone concentration.
103 For example, Tai et al. (2013) found that LULCC projections in the
104 Intergovernmental Panel on Climate Change (IPCC) A1B scenario with widespread
105 crop expansion could reduce isoprene emission by ~10% globally compared with the
106 land use and land cover at present. Such a reduction could correspondingly lead to an
107 up to 4 ppbv of ozone decrease in the eastern US and western Europe, and an up to 6
108 ppbv increase in South and Southeast Asia, whereby the difference in the sign of
109 responses is driven primarily by the different ozone production regimes.

110 Dry deposition is another key factor modulating ozone (e.g., Wesely, 1989;
111 Val Martin et al., 2014; Lin et al., 2019). Dry deposition is the most efficient over
112 densely vegetated regions via the stomatal uptake of ozone and its precursors, and
113 LULCC can alter these fluxes. Kroeger et al. (2013) found that reforestation over
114 peri-urban areas in Texas, USA, could effectively enhance dry deposition, resulting in

115 decreases in ozone and its precursors. Fu and Tai (2015) found that LULCC driven by
116 climate and CO₂ changes could overall enhance dry deposition and decrease ozone by
117 up to 4 ppbv in East Asia during the past three decades. The dry deposition
118 enhancement mostly arises from climate- and CO₂-induced increase in leaf area index
119 (LAI), which more than offsets the compensating effect of cropland expansion (Fu
120 and Tai, 2015). The relative importance of isoprene emission and dry deposition,
121 which could have counteracting effects on ozone given the same LULCC, is strongly
122 dependent on local NO_x concentrations and vegetation type (Wong et al., 2018).

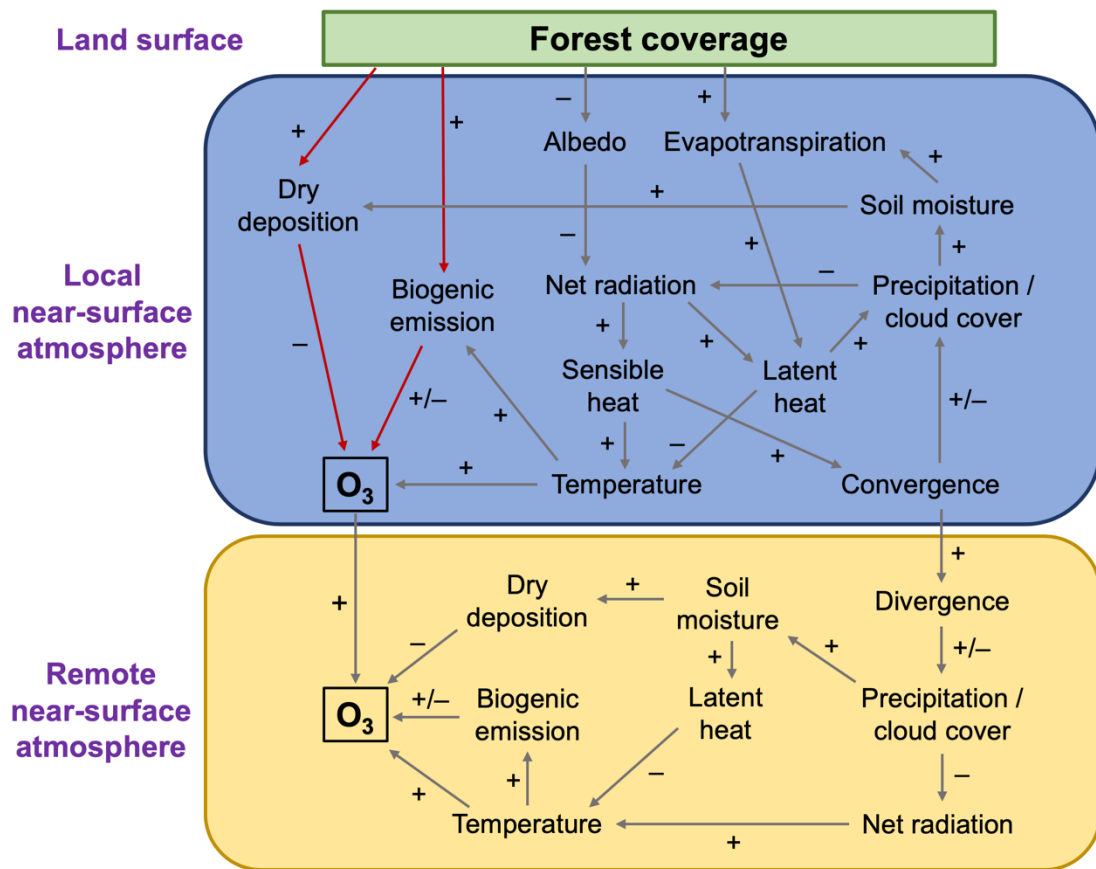
123 LULCC can also affect weather and climate by perturbing the biosphere-
124 atmosphere exchange of water and energy fluxes (e.g., Betts, 2001; Bonan, 2016;
125 Pitman et al., 2009). For example, afforestation generally cools the surface in tropical
126 regions, where evaporative cooling generally exceeds radiative warming from
127 reduced albedo, but warms the surface in boreal forests due to the more dominant
128 radiative warming effect (e.g., Arora and Montenegro, 2011; Lee et al., 2011; Bonan,
129 2008). There is little consensus on the effects of afforestation in midlatitude regions
130 (e.g., Boisier et al., 2012; de Noblet-Ducoudré et al., 2012). Recent studies (Devaraju
131 et al. 2015; Laguë and Swann 2016) have identified that LULCC in midlatitude
132 regions can modify the global energy balance, impacting cloud cover, precipitation,
133 and circulation pattern. Furthermore, the impacts of such surface forcing could extend
134 into the upper troposphere, alter large-scale circulation pattern, and consequently
135 affect the climate in remote regions (Henderson-Sellers et al. 1993; Chase et al., 2000;
136 Swann et al., 2012; Medvigy et al., 2013). Laguë et al. (2019) examined the climatic
137 effects of individual physical components in the land surface (albedo, evaporative
138 resistance and surface roughness), and found that temperature responds most to
139 changes in albedo and evaporative resistance through large-scale atmospheric

140 feedbacks. Still, how individual land characteristics play out together and interact
141 with each other to affect the atmospheric general circulation are not fully understood.

142 By and large, the impacts of LULCC on weather and climate are complex.
143 There is high confidence that LULCC can affect regional climate and climate in
144 remote areas as far as few hundreds of kilometers away (Jia, et al., 2019). The
145 magnitude and sign of regional climate change vary across regions depending on the
146 magnitude of LULCC and background climatic conditions. However, on the global
147 scale, the net changes resulting from LULCC alone are relatively small (e.g.,
148 Matthews et al. 2004; Pongratz et al. 2010; Brovkin et al., 2013; Shevliakova et al.
149 2013; Simmons and Matthews, 2016). Thus, sometimes climatic responses to LULCC
150 may be difficult to distinguish from natural climate variability especially on the global
151 scale.

152 The modification of the overlying meteorological environment and climate
153 induced by LULCC and the associated exchange of momentum, heat and moisture
154 between the land and atmosphere can be defined as “biogeophysical effects” of
155 LULCC. Such effects can further alter surface ozone on local to pan-regional scales
156 (Jiang et al., 2008; Ganzeveld et al., 2010; Wu et al., 2012), and we shall call these
157 and related pathways the biogeophysical effects of LULCC on ozone. In particular, a
158 LULCC-induced increase in surface temperature could (1) accelerate peroxyacetyl
159 nitrate (PAN) decomposition into NO_x (Jacob and Winner, 2009; Doherty et al., 2013;
160 Pusede et al., 2015), (2) increase biogenic VOCs emissions from vegetation
161 (Guenther et al., 2012; Wang et al., 2013; Squire et al., 2014), and (3) lead to more
162 water vapor in air that tends to increase ozone destruction (Jacob and Winner, 2009).
163 The net effect of higher temperatures is almost always ubiquitously an enhancement
164 of ozone levels reported from both observational (e.g., Porter et al., 2015; Pusede et

165 al., 2015) and modeling (e.g., Shen et al., 2016; Lin et al., 2017) studies in many
 166 polluted regions. Meanwhile, any reduction in precipitation, cloud cover and soil
 167 moisture can also enhance surface ozone because of the associated increase in solar
 168 radiation and reduced dry deposition velocity. Fig. 1 summarizes the possible
 169 biogeochemical and biogeophysical pathways through which a change in forest
 170 coverage may influence surface ozone. The relative importance of different pathways,
 171 many of which may either counteract or amplify each other, is strongly dependent on
 172 forest types.
 173



174
 175 Figure 1. Schematic diagram showing the biogeochemical and biogeophysical effects of any changes in
 176 the forest cover resulting from land use and land cover change (LULCC) on surface ozone. Red arrows
 177 indicate the biogeochemical pathways and grey arrows indicate the biogeophysical effects via changes
 178 in the overlying meteorological environment. The sign associated with each arrow indicates the
 179 correlation between the two variables; the sign of the overall effect (positive or negative) of a given

180 pathway is the product of all the signs along the pathway. We here focus on processes initiated on the
181 land surface by LULCC, and the corresponding responses in local near-surface atmosphere (blue box)
182 and remote near-surface atmosphere (yellow box).

183

184 The LULCC biogeophysical effects have thus far been largely unexplored,
185 though biogeochemical effects of LULCC have been examined by a number of
186 studies (Wu et al., 2012; Fu and Tai, 2015; Heald and Geddes, 2016). Only a few
187 recent studies have implicitly included such biogeophysical effects of LULCC in their
188 coupled land-atmosphere models when assessing the impacts of LULCC on surface
189 ozone. Val Martin et al (2015) studied the combined effects of LULCC on surface
190 ozone using future LULCC scenarios, and found an increase of 2–3 ppbv from 2000
191 to 2050 over US national parks. Ganzeveld et al. (2010) also calculated the future
192 LULCC from 2000 to 2050, and found that an increase in boundary-layer ozone
193 mixing ratios by up to 20% over the tropics. However, these studies did not
194 distinguish between the roles of biogeophysical vs. biogeochemical effects, or
195 decipher the physics and relative importance of various mechanisms behind the
196 combined effects.

197 The aim of this study is to investigate how and to what extent global LULCC
198 could affect surface ozone in the near future by investigating and distinguishing
199 between the biogeochemical, biogeophysical and combined effects of LULCC. We
200 suggest a new line of biogeophysical pathways linking LULCC to surface ozone, and
201 also consider biogeochemical pathways through isoprene emission and dry deposition
202 changes caused by LULCC. In particular, over the regions without significant
203 LULCC but showing substantial ozone changes, we find that the biogeophysical
204 effects arising from LULCC-induced atmospheric circulation changes can be
205 dominant and could be isolated from the combined effects. LULCC is one of the key

206 strategies for climate change mitigation, but meanwhile has substantial impacts on
207 ozone pollution. Understanding its comprehensive pathways on surface ozone can
208 help provide important references for integrated air quality and land use management
209 in the future.

210 **2. Data and methods**

211 *2.1 Modeling framework*

212 To simulate the impacts of LULCC on surface ozone, we use the Community
213 Earth System Model (CESM) version 1.2 (<http://www.cesm.ucar.edu/models/>), which
214 is a comprehensive global model that couples different independent components for
215 the atmosphere, land, ocean, sea ice, land ice and river runoff (Lamarque et al., 2012).
216 The atmospheric component is the Community Atmosphere Model version 4
217 (CAM4), which uses a finite-volume dynamical core with comprehensive
218 tropospheric and stratospheric chemistry (CAM-Chem). Chemical mechanisms are
219 based on the Model for Ozone and Related chemical Tracers (MOZART) version 4
220 (Emmons et al., 2010). For the land component, the Community Land Model (CLM)
221 version 4.5 (Oleson, 2013) considers 16 Plant Function types (PFTs) (Lawrence et al.,
222 2011), and prescribes the total leaf area index (LAI), the PFT distribution and PFT-
223 specific seasonal LAI derived from Moderate Resolution Imaging Spectroradiometer
224 (MODIS) observations. We use the Satellite Phenology (SP) mode of CLM4.5 for all
225 simulations, which prescribes vegetation structural variables including LAI and
226 canopy height; active biogeochemical cycling in terrestrial ecosystems is not turned
227 on.

228 In CLM4.5, biogenic VOC emissions are computed using the Model of
229 Emissions of Gases and Aerosols from Nature (MEGAN) version 2.1 (Guenther et al.,
230 2012), accounting for the major known processes controlling biogenic VOC

231 emissions from terrestrial ecosystems, such as effects of temperature, solar radiation,
232 soil moisture, leaf age, CO₂ concentrations, and vegetation species and density.
233 Biogenic VOC emissions in MEGAN are allowed to respond interactively to changes
234 of these processes. Thus, isoprene emission is allowed to respond to spatiotemporal
235 changes in PFTs and the associated changes in meteorological conditions in this
236 study. Dry deposition of gases and aerosols are computed based on the multiple
237 resistance approach of Wesely (1989), updated by Emmons et al. (2010), Lamarque et
238 al. (2012) and Val Martin et al. (2014). In the scheme, dry deposition velocity is the
239 inverse of aerodynamic resistance (R_a), sublayer resistance (R_b) and bulk surface
240 resistance (R_c), whereby R_c includes a combination of resistances from vegetation
241 (including stomatal resistance), lower canopy, and ground with specific values for
242 different land types. Correspondingly, dry deposition velocity in the scheme responds
243 to primarily meteorological and ecophysiological conditions. Soil NO_x emissions are
244 dependent on soil moisture, soil temperature and vegetation cover (Emmons et al.,
245 2010; Yienger and Levy, 1995), while biomass burning emissions and anthropogenic
246 emissions of ozone precursors, are prescribed by inventory at present-day levels.

247 The coupled CAM-Chem-CLM model configuration of CESM can be run
248 with prescribed meteorology to drive atmospheric chemistry-only simulations
249 (hereafter as dynamical Off-line mode), or with interactive, dynamically simulated
250 meteorology using CAM4 (hereafter as On-line mode). These two modes are both
251 applied in the study. In particular, the Off-line mode is used to quantify the
252 biogeochemical effects of LULCC alone on surface ozone in the absence of any
253 associated meteorological responses to LULCC. The On-line mode is applied to
254 assess the biogeophysical and combined effects on ozone caused by LULCC,
255 considering also the effects of the resulting meteorological changes.

256 For the Off-line mode, we use the Goddard Earth Observing System Model
257 Version 5 (GEOS-5) (<https://rda.ucar.edu/datasets/ds313.0/>) (Tilmes, 2016)
258 assimilated meteorology as the driving fields, with a horizontal resolution of
259 $1.9^{\circ} \times 2.5^{\circ}$ and 56 vertical levels between the surface and the 4-hPa level. For the On-
260 line mode of CAM4-Chem-CLM, 26 vertical levels are used between the surface and
261 4 hPa, with the same horizontal resolution as the Off-line mode. For all simulations,
262 concentrations of long-lived greenhouse gases including CO₂, CH₄, and N₂O are
263 prescribed at present-day. For the anthropogenic emissions used for all simulation are
264 described in Lamarque et al. (2010, 2012) and references therein. Climatic changes
265 that may arise from land cover disturbances of the terrestrial carbon and nitrogen
266 cycles are not the focus of this study, which aims to delineate the more immediate
267 responses of surface ozone to LULCC.

268 The CAM-Chem-simulated atmospheric chemistry has been extensively
269 evaluated and documented (e.g., Lamarque et al., 2012). In general, CAM-Chem can
270 reasonably replicate observed values at individual sites (CASTNET for US and
271 EMEP for Europe) (Lamarque et al., 2012; Val Martin et al., 2014; Sadiq et al.,
272 2017), and mid- and upper-tropospheric distribution derived from a compilation of
273 ozone measurements (Lamarque et al., 2010; Cooper et al., 2010), albeit with a
274 general overestimation. The performance is comparable to other global and regional
275 models (Lapina et al., 2014; Parrish et al., 2014). Uncertain emissions, coarse
276 resolution (Lamarque et al., 2012), misrepresentation of dry deposition process (Val
277 Martin et al., 2014) and overestimation of stomatal resistance (Lin et al., 2019) are all
278 likely factors contributing to the biases.

279

280 2.2 *Present and future land use and land cover scenarios*

281 For the present-day land cover distribution, satellite phenology based on
282 MODIS and a cropping dataset from Ramankutty et al. (2008) are used (see Lawrence
283 et al., 2011). The cropping dataset combines agricultural inventory data and two
284 satellite-derived land products. For the future land cover, projections based on the
285 Representative Concentration Pathways (RCP) 4.5 and 8.5 scenarios are adopted (van
286 Vuuren et al., 2011). Both are computed using Integrated Assessment Models (IAM)
287 for the Phase 5 of the Coupled Model Intercomparison Project (CMIP5) community,
288 incorporating anthropogenic transformation and activities associated with carbon
289 releases (e.g., wood harvest). These LULCC projections are internally consistent with
290 the corresponding emission scenarios and development pathways for the Fifth
291 Assessment Report (AR5) of Intergovernmental Panel on Climate Change (IPCC)
292 (Taylor et al., 2012). In general, the RCP4.5 LULCC has the most extensive use of
293 land management as a carbon mitigation strategy, with the expansion of forest areas
294 combined with large reductions in croplands and grasslands. The RCP8.5 LULCC has
295 the least effective use of land management for carbon mitigation, with large
296 expansion in both croplands and grasslands together with substantial forest losses. In
297 this study, anthropogenic emissions are held constant at the present-day level for all
298 runs, thus the effects of LULCC can be considered as being decoupled from changes
299 in anthropogenic emissions in order to isolate the effects of LULCC alone.

300 Both present-day and future land cover are transformed into PFTs changes for
301 implementation into CESM (Lawrence et al., 2012; Oleson et al., 2013). The long-
302 term time series of LULCC span through the historical (1850–2005) and future
303 (2006–2100) periods in 5-year intervals (Riahi et al., 2007; van Vuuren et al., 2007;
304 Wise et al., 2009a), and are then interpolated and harmonized with smooth transitions

305 on the annual timescale (Hurtt et al., 2011). For this work, we focus on LULCC from
306 the present-day (2000) to future (2050) period.

307

308 *2.3 Model experiments*

309 We have two sets of configuration, Off-line mode and On-line mode to
310 investigate the impacts of LULCC on surface ozone (see Table 1). We focus on boreal
311 summer month (June-July-August, JJA) averages as this is the period when ozone
312 pollution is generally the most severe in the Northern Hemisphere. In the first set of
313 simulations in Off-line mode, surface ozone would respond to LULCC only through
314 biogeochemical effects that mainly include changes in dry deposition velocity and
315 isoprene emissions without meteorological responses to LULCC. The Off-line mode
316 includes control run (Off-line_CTL) using present-day (year 2000) distribution of
317 land use and land cover, and two future simulations Off-line_45 and Off-line_85, with
318 year-2050 land use and land cover distribution following RCP4.5 and RCP8.5,
319 respectively. All three experiments are time-sliced simulations using prescribed
320 GEOS-5 meteorology from 2004 to 2017 for 14 years allowing for interannual
321 climate variability, and we use the last 10-year averages for analysis. The statistical
322 significance of the comparison amongst these experiments was assessed by the
323 Student's t-test at the 95% confidence levels.

Case Name	Land treatment	Meteorology	Simulated years	Model forcing	
1	Off-line_CTL	Present-day (2000) land use and land cover (LULC) map	GEOS-5 reanalysis (2004-2017)	14 years, the last 10 years for analysis	- Present-day (2000) well-mixed greenhouse gases and short-lived gases and aerosols, anthropogenic emissions;
2	Off-line_45	2050 RCP4.5 future LULC map as a time slice	Same as above	Same as above	- Present-day (2000) monthly mean sea surface temperature and sea ice
3	Off-line_85	2050 RCP8.5 future LULC map as a time slice	Same as above	Same as above	- All simulations use the SP mode in CLM
4	On-line_CTL	Present-day (2000) LULC map	Simulated online	60 years (looped over same year of forcing), the last 30 years for analysis	- Isoprene emission is from MEGAN
5	On-line_45TS	2050 RCP4.5 future LULC map as a time slice	Same as above	Same as above	- Dry deposition velocity is based on Wesely (1989) updated by Val Martin et al. (2014)
6	On-line_85TS	2050 RCP8.5 future LULC map as a time slice	Same as above	Same as above	
7, 8	On-line_45 ^a	2000-2005 historical, 2006-2065 RCP4.5 transient LULC map	Same as above	66 years (transient land forcing all the way), the last 30 years ^c for analysis	
9, 10	On-line_85 ^b	2000-2005 historical, 2006-2065 RCP8.5 transient LULC map	Same as above	Same as above	

325

326 Table 1. List of model experiments. ^{a, b} Case 8 and 10 are in On-line_45 and On-line_85 are similar to

327 Case 7 and 9, respectively, but with slightly different initial conditions to produce two ensemble

328 members. ^c The analysis time period is from 2036 to 2065, centered around year 2050, as part of the
329 transient land forcing.

330

331 In the second set of On-line mode simulations, ozone would respond to both
332 the biogeochemical and biogeophysical effects caused by future projected LULCC.
333 The first experiment On-line_CTL, reflects present-day conditions and uses land
334 surface forcing for year 2000. The second and third experiments, On-line_45TS and
335 On-line_85TS, are time-sliced simulations using 2050 land cover distribution
336 following RCP4.5 and RCP8.5, respectively. These two experiments are designed for
337 direct, parallel comparison with the Off-line simulations, except with longer
338 integration (60 years) and analysis (30 years) time to capture interannual climate
339 variability. Because these multi-year simulations are looped over the same year of
340 land cover forcing, they can be considered as a quasi-ensemble run and the multi-year
341 average can be considered as the ensemble average. The fourth and fifth experiments,
342 referred to as On-line_45 and On-line_85, are transient simulations performed
343 continuously from year 2000 to 2065 using transient land cover maps projected for
344 the RCP4.5 and RCP8.5 scenarios, respectively. These On-line transient simulations
345 are repeated by a series of ensemble runs with slightly different initial conditions,
346 with two ensemble members for each scenario. All the On-line experiments analysis
347 is based on the last 30-year average and the ensemble average when modeled
348 variables have attained a quasi-steady state. Comparison between the time-sliced and
349 transient simulations helps us ascertain the strengths of LULCC-induced climate
350 signals.

351 All simulations are performed with prescribed sea surface temperature and
352 sea-ice cover following the HadISST data set (Rayner et al., 2003) at the year-2000

353 level. Long-lived greenhouse gases and thus the radiative forcing from them are kept
354 at present-day conditions (year 2000) to isolate the effects of LULCC only.

355 These model configurations allow us to separate and examine: (1)
356 biogeochemical effects of LULCC on surface ozone, (2) biogeophysical effects on
357 surface ozone, and (3) the combined effects induced by LULCC on surface ozone and
358 its precursors and dry deposition.

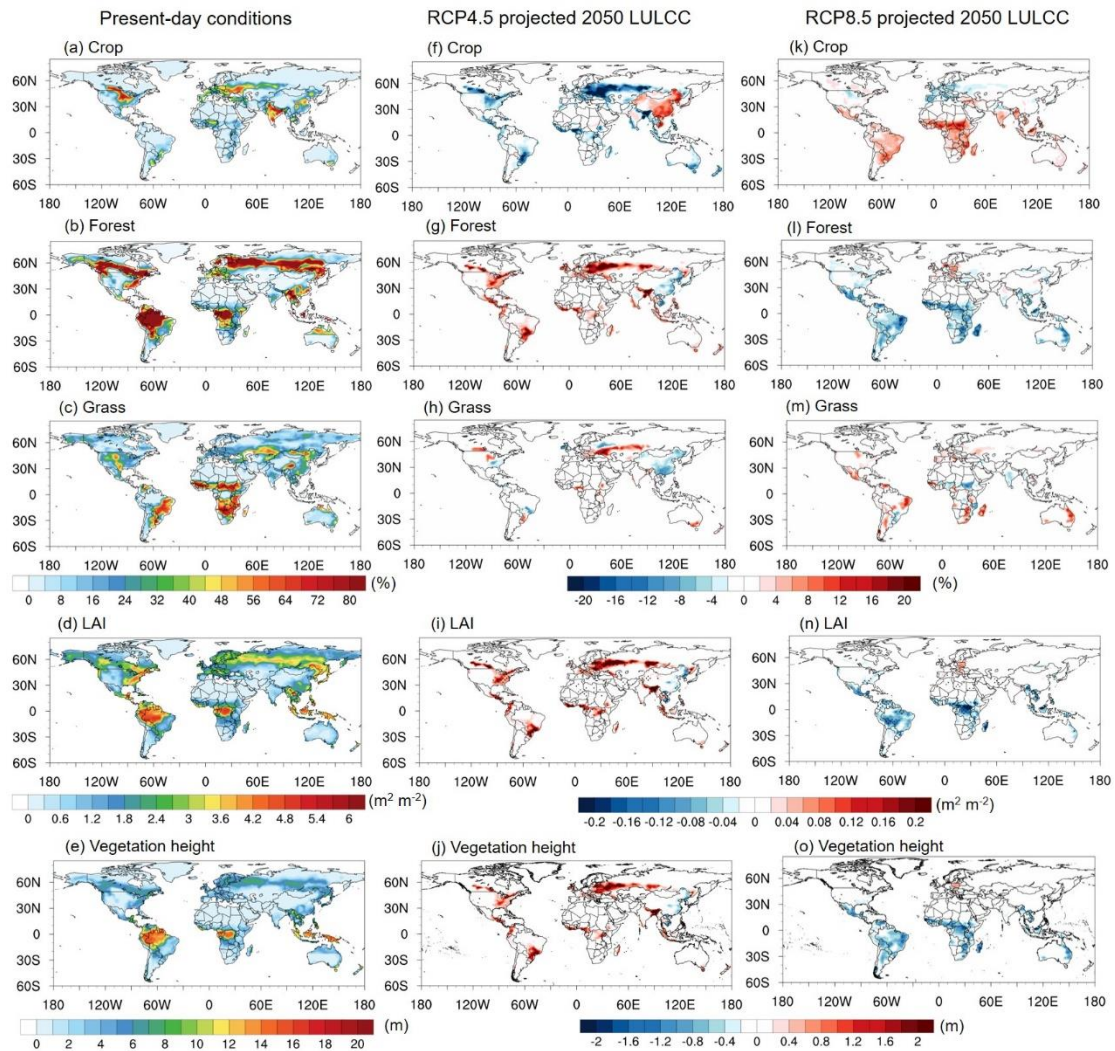
359

360 **3. Results**

361 *3.1 Projected land use and land cover change from 2000 to 2050*

362 Figure 2 shows the global distribution of present-day (year 2000) PFTs and
363 future projected changes (2000 to 2050) following RCP4.5 and RCP8.5 for three
364 major land cover categories. The future LULCC in RCP4.5 is characterized by
365 extensive forest expansion (Figs. 2f, g). Transition from present-day to 2050 in
366 RCP4.5 highlights the global growth of forest from 71.8 million to 74.0 million km²,
367 at the expense of croplands (from 14.7 million to 12.3 million km²); grasslands
368 slightly increase in area from 33.7 million to 33.8 million km². The net increase of 2.2
369 million km² of forests is consistent with that provided by Hurtt et al. (2011),
370 Lawrence et al. (2012) and Heald and Geddes (2016). Fig. 2f also illustrates cropland
371 area increases over Southeast Asia, India and China. Such increases are due to more
372 bioenergy crop production for the purpose of climate change mitigation, economic
373 advantages from agriculture productivity growth, lower regional land prices, and
374 availability of undeveloped lands in these developing regions (Wise et al., 2009b;
375 Thomson et al., 2011). In contrast, regions such as Europe, US and Canada, undergo
376 extensive reforestation. RCP8.5 LULCC is characterized by extensive cropland
377 expansion (Figs. 2k, l, m), driven mainly by a large increase in the global population

378 and a slow increase in crop yields due to a slow rate of exchange of technology
 379 globally (Riahi et al., 2011). Cropland expansion occurs largely over the tropical belt
 380 (30°N-30°S) at the expense of forest reduction. The total increases in croplands are by
 381 1.8 million km², and forest area decreases by 2.5 million km².



382
 383 Figure 2. Present-day (2000) land use and land cover by percentage of land coverage, total leaf area
 384 index (LAI) and vegetation height (left), and their changes from 2000 to 2050 under RCP4.5 (middle)
 385 and RCP8.5 (right) scenarios for the boreal summer (June-July-August) (units at the right side of the
 386 color bar). Plant function types (PFTs) in CESM are here grouped into three major categories: crop,
 387 forest and grass. The treatment of vegetation including PFT fractional coverage, LAI and vegetation
 388 height is prescribed using the SP mode of CLM4.5 in both the present-day case and future LULCC
 389 scenarios. For the future cases, PFT fractional coverage is derived according to the RCP land scenarios.
 390

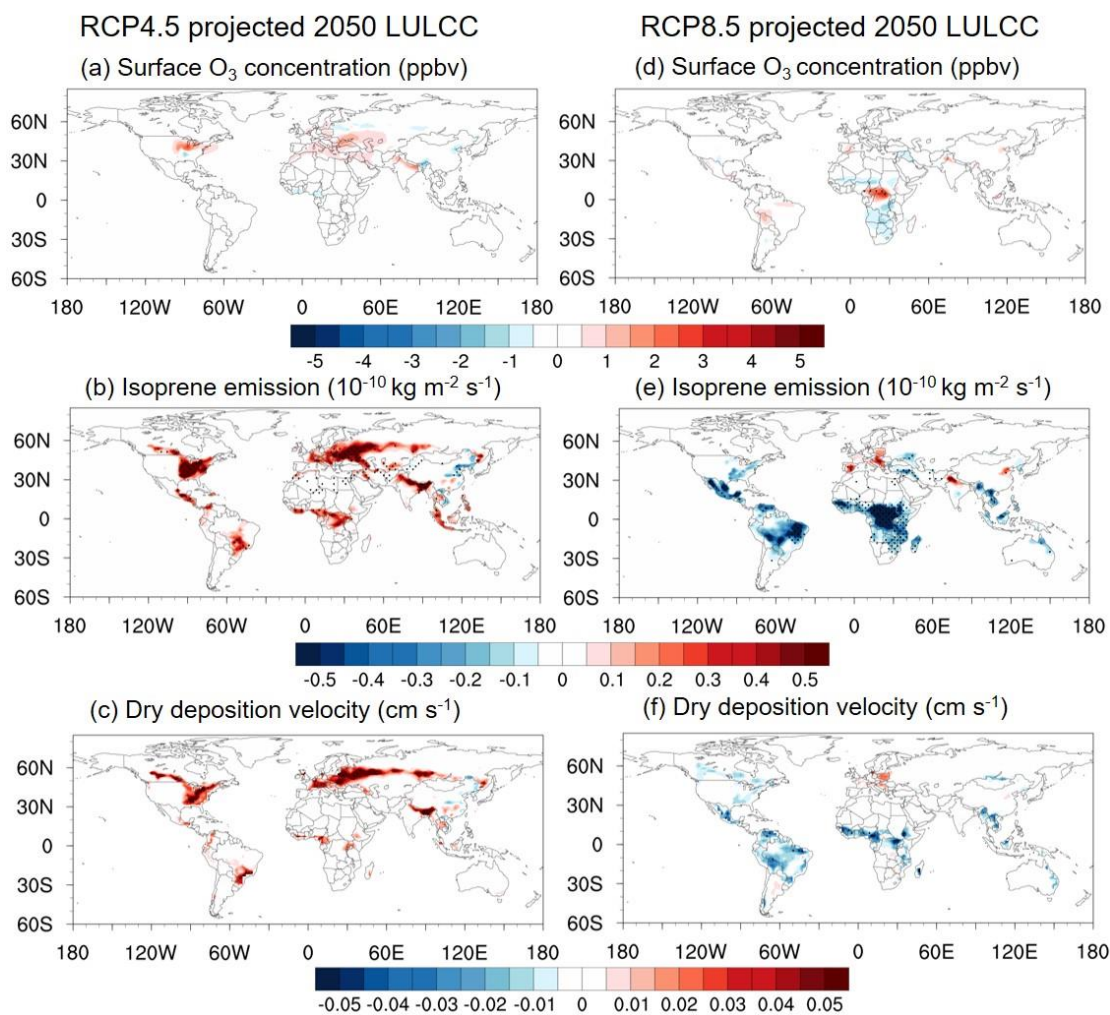
391 The present-day LAI and its changes associated with the future projected
392 LULCC are shown in Figs. 2d, 2i and 2n. Forest expansion leads to increases in LAI,
393 whereas deforestation results in LAI reduction. For RCP4.5, due to the widespread
394 reforestation and afforestation except in East Asia, LAI increases significantly.
395 Particularly over Europe and the US, the absolute increase in LAI is > 0.1 . For
396 RCP8.5, LAI generally declines with intense reductions over the tropical regions.

397

398 *3.2 Biogeochemical effects of land use and land cover change on surface ozone*

399 Figure 3 shows the simulated changes in ozone concentrations, isoprene
400 emission rates and dry deposition velocities based on the Off-line simulations. We
401 find that isoprene emission changes correspond closely with the LULCC in each
402 future scenario from 2000 to 2050 (Figs. 3b, e). For RCP4.5, isoprene emission
403 increases over the regions with forest expansion, including the US, Europe and some
404 tropical regions, but decreases over East Asia. Such isoprene emission increases are
405 primarily driven by forest expansion, since forest PFTs typically emit much more
406 isoprene than crops and grasses (Guenther et al., 2012). For RCP8.5, isoprene
407 emission decreases over the tropics with slight increases over Europe, north China
408 and north India, largely due to forest reduction in this scenario.

409



410

411 Figure 3. Simulated 2000-to-2050 changes in surface ozone, isoprene emission, and dry deposition
 412 velocity under RCP4.5 and RCP8.5 projected LULCC for the boreal summer (June-July-August)
 413 averaged for the final 10 years of simulations. Regions with dots indicate changes that are significant at
 414 the 95% confidence level. These are results from Off-line runs with prescribed meteorology; i.e.,
 415 meteorological variables do not respond to LULCC.

416

417 Table 2 summarizes the percentage and absolute changes of the annual global
 418 isoprene emission. The simulated present-day annual global isoprene is $353.8 \text{ Tg C yr}^{-1}$, in the middle of the range $308\text{--}678 \text{ Tg C yr}^{-1}$ summarized by Guenther et al.
 419 yr^{-1} , in the middle of the range $308\text{--}678 \text{ Tg C yr}^{-1}$ summarized by Guenther et al.
 420 (2012). For the RCP4.5 LULCC, the annual global isoprene emission increases by
 421 5.2%, but it decreases by 11.8% for RCP8.5. The isoprene emission changes are in
 422 line with these studies by Heald et al. (2008) and Wu et al. (2012), who estimated a

423 decrease of 12–15% in global isoprene emission under the net biogeochemical effect
 424 of future LULCC (A1B and A2 scenarios).

425

		Isoprene emissions (TgC yr ⁻¹)	% change	Ozone dry depositional sink (Tg yr ⁻¹)	% change	Ozone concentration (ppbv)	% change
	Off-line_CTL	353.8		886.8		23.6	
Off- line	Off-line_45	372.3	5.2	895.4	1.0	23.7	0.4
	Off-line_85	311.9	-11.8	879.8	-0.8	23.5	-0.4
	On-line_CTL	417.7		969.2		26.2	
	On-line_45TS	435.4	4.3	974.7	0.6	26.5	1.2
On- line	On-line_85TS	386.8	-7.4	964.1	-0.5	26.4	0.8
	On-line_45	440.3	5.5	975.6	0.6	26.6	1.5
	On-line_85	385.2	-7.7	964.1	-0.5	26.3	0.4

426 Table 2. Annual average global isoprene emission and ozone dry-depositional sink as influenced by
 427 future LULCC in the RCP4.5 and RCP8.5 scenarios; shown separately are changes in prescribed
 428 meteorology (biogeochemical effects only) and coupled atmosphere-chemistry-land configurations
 429 (both biogeochemical and biogeophysical effects).

430

431 Fig. 3c shows that LULCC in the RCP4.5 scenario has enhanced dry
 432 deposition velocity over most regions where forests have expanded. Forest with both
 433 large LAI, and high surface roughness often provides the highest dry deposition
 434 velocity amongst all PFTs (Emmons et al., 2010; Lamarque et al., 2012). The most
 435 dramatic changes occur in Europe where local maximum changes occur in land cover
 436 between forests and croplands. Local decreases over East Asia are the result of
 437 deforestation. For RCP8.5, dry deposition velocity decreases mostly over the regions
 438 where tropical forests are replaced by croplands (Fig. 3f). Equatorial Africa and the
 439 Amazon experience the largest decrease in dry deposition velocity relative to present-

440 day conditions. Some increases over Western Europe are the result of local
441 reforestation.

442 The globally averaged change in the dry-depositional sink is around 1%
443 (Table 2). Local dry deposition velocity changes within 0.05 cm s^{-1} . The value of dry
444 deposition velocity change is in line with previous studies exploring future 2050
445 LULCC alone on the dry deposition velocity of ozone (e.g., Verbeke et al., 2015),
446 though our results show slightly larger changes due to larger LAI differences between
447 forests and crops/grasses during the boreal summer compared with their annual mean
448 values of differences from Verbeke et al. (2015).

449 Figs. 3a and 3d show the impacts of future projected LULCC on surface
450 ozone. LULCC under RCP4.5 with massive forest expansion increases isoprene
451 emission that could increase surface ozone, but also enhance dry deposition velocity
452 that could reduce surface ozone. The overall changes in surface ozone are thus
453 generally small due to these compensating effects. There are a few regions with
454 surface ozone changes by up to 2 ppbv. In particular, over the US, opposite surface
455 ozone changes are seen in RCP4.5: an increase in the northeast US and a decrease in
456 the southeast US despite of the fact that both changes are driven by forest expansion
457 (Fig. 3a). Such a contrasting pattern is shaped by the local atmospheric chemical
458 conditions related to $\text{O}_3\text{-NO}_x\text{-VOC}$ chemistry. The northeast US is a high- NO_x region,
459 and increases in isoprene emission result in enhanced ozone, more than offsetting the
460 effect of increasing dry deposition velocity. In contrast, the southeast US is a high-
461 isoprene-emitting region; additional isoprene may react with ozone and NO_x , thereby
462 suppressing surface ozone production (Kang et al., 2003; von Kuhlmann et al., 2004;
463 Fiore et al., 2005; Pfister et al., 2008). Furthermore, in the low- NO_x region, OH is
464 largely removed by reactions with biogenic VOCs, producing peroxy radicals that

465 form HO₂ or producing organic peroxides. Recent studies found that these peroxides
466 can be rapidly photolyzed, making them at best a temporary HO_x reservoir (e.g.,
467 Thornton et al., 2002; Kubistin et al., 2010). This result implies that in low-NO_x
468 regions ozone production may be NO_x-saturated more often than current models
469 suggest. Suppressed ozone is also found in the tropical regions of South America and
470 Africa (Fig. S1a). Together with the increase in dry deposition velocity, overall there
471 is a decrease of surface ozone. Similar to the northeastern US conditions, southern
472 Europe, northeastern India and northern China are also high-NO_x regions.

473 Under the RCP8.5 scenario with substantial cropland and grassland expansion,
474 decrease in isoprene emission and dry deposition again offset each other in
475 controlling surface ozone in high-NO_x regions. Surface ozone concentration decreases
476 by around 1 ppbv over the north-central and southern Africa, but increases by up to 2
477 ppbv over equatorial Africa and central South America (Fig. 3d). In particular, the
478 area with enhanced ozone in these regions corresponds well with reductions in
479 isoprene emission and dry deposition together. Equatorial Africa is a high-isoprene-
480 emitting, low-NO_x region, thus decreases of isoprene emission together with reduced
481 dry deposition would lead to enhanced ozone (Fig. S1b).

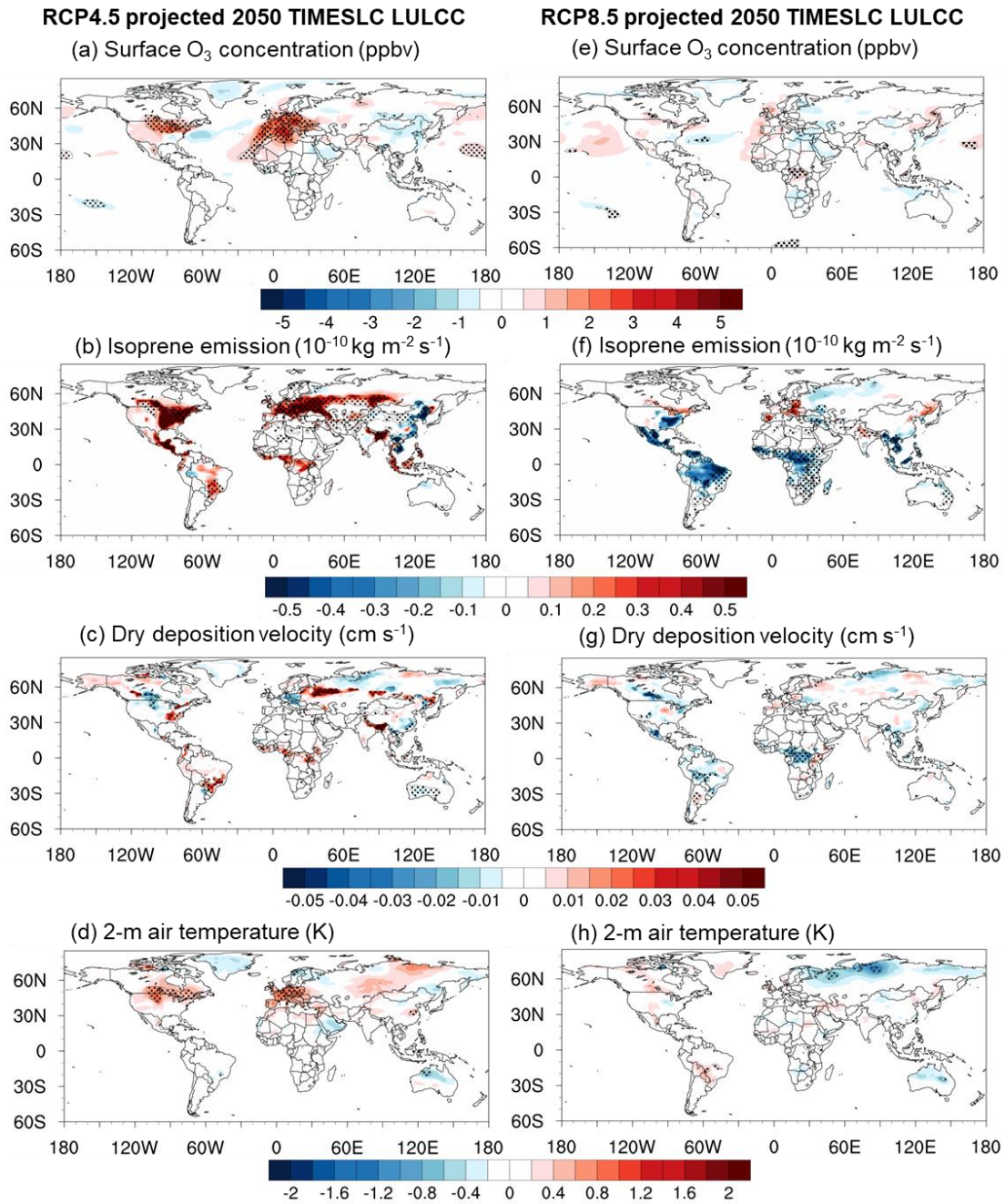
482

483 *3.3 Biogeophysical effects of land use and land cover change on surface ozone*

484 Next, we examine results from the On-line simulations, which allow us to
485 assess the impacts of LULCC on surface ozone when the overlying meteorological
486 environment is also modified by LULCC. Fig. 4 shows the simulated changes in
487 ozone concentrations, isoprene emissions rates, dry deposition velocities as well as 2-
488 m air temperature from the On-line time-sliced simulations. The simulated changes in
489 surface ozone is in the range from -2 to +5 ppbv (Figs. 4a, e). The magnitude of

490 ozone changes in On-line simulations is overall larger than those in Off-line
491 simulations (Fig. 3 and Table 2), which consider biogeochemical effects only,
492 indicating the importance of complications from the changing meteorological
493 environment in response to LULCC. Within the On-line simulations, more substantial
494 responses of meteorology as well as of surface ozone to LULCC are found in RCP4.5
495 compared with those in RCP8.5.

496 In contrast to the clear, localized signals in ozone changes in response to
497 LULCC through biogeochemical pathways, surface ozone changes are more complex
498 when biogeophysical pathways are also involved (Figs. 4a, e). Most importantly, both
499 local and remote ozone changes can be discerned. Such signals are not captured by
500 the Off-line simulations in which changes only respond to LULCC locally (Fig. 3).
501 Furthermore, changes in 2-m air temperature are found to be correlated well with
502 patterns of changes in ozone (Fig. S2a, d), indicating that the biogeophysical drivers
503 that modify meteorological conditions may play critical roles in ozone changes. Figs.
504 4d and 4h show simulated changes in 2-m air temperature before and after LULCC.
505 Regional-scale temperature changes of up to 2 K are found. Such magnitudes of
506 temperature anomalies induced by LULCC are in line with those from previous
507 experiments (Lawrence et al., 2012; Brovkin et al., 2013). Over the regions where
508 temperature increases, surface ozone increases correspondingly.



509

510

511 Figure 4. Simulated 2000-to-2050 changes in surface ozone, isoprene emission, dry deposition
 512 velocity and 2-m air temperature for the boreal summer averaged over the 30-year analysis window,
 513 under two future scenarios (RCP4.5 and RCP8.5) of LULCC. Regions with dots indicate changes that
 514 are significant at the 95% confidence level. These results are from the On-line runs (land forcing 2050
 515 minus 2000) with dynamic meteorological responses to LULCC from time-sliced simulations On-
 516 line_45TS and On-line_85TS (Table 1).

517

518 Changes in isoprene emission also correlate with temperature changes (Figs.
519 4b, d; Figs. 4f, h, Fig. S2b). Isoprene emission also increases in regions with forest
520 expansion, reflecting not only the biogeochemical effects due to higher fractional
521 coverage of isoprene-emitting vegetation types (Section 3.2), but also the
522 biogeophysical effects arising from changing 2-m air temperature.

523 Changes in dry deposition velocity (Figs. 4c, g, Fig. S2c) also correlate to
524 meteorological changes. In the dry deposition scheme, stomatal resistance can
525 respond to atmospheric dryness and soil water stress. For instance, drier conditions
526 are captured in RCP4.5 in the north-central US as initiated by the LULCC further
527 east, with anomalous moisture divergence (Fig. 5n) and soil moisture (Fig. 5o). The
528 drier conditions could result in suppressed dry deposition in the corresponding regions
529 (Fig. 5c). The responses of dry deposition to drought conditions have also been
530 observed by recent studies (e.g., Lin et al., 2019). Furthermore, changes in surface
531 roughness can influence aerodynamic resistance and thus dry deposition via
532 modifying boundary-layer turbulence. In LULCC scenarios, surface roughness is
533 modified substantially with increases in RCP4.5 (Fig. 2j) and reductions in RCP8.5
534 (Fig. 2o), which generally decrease (increase) resistance and enhance (decrease) dry
535 deposition in RCP4.5 (RCP8.5) in LULCC regions, though the overall changes in dry
536 deposition is dominantly shaped by the combined meteorological effects of LULCC.

537 Table 2 shows in general, the percentage changes in isoprene emission and dry
538 deposition in the On-line simulations are smaller than in the Off-line simulations in
539 both scenarios, reflecting that on a global scale, LULCC-induced meteorological
540 changes partly offset the biogeochemical effects of changing land cover types on
541 ozone.

542 Thus, changes in ozone can be caused by both biogeochemical and
543 biogeophysical effects of LULCC; furthermore, both effects are highly coupled with
544 each other. We find that in particular the biogeophysical effects of LULCC play
545 critical roles in modulating surface ozone. Hereafter, we focus on the broad regions of
546 North America and Europe, in order to elucidate the origins of surface ozone changes
547 in response to LULCC-induced meteorological changes. We also focus on RCP4.5
548 only, because no significant changes in ozone or other meteorological variables are
549 found for the RCP8.5 LULCC scenario.

550

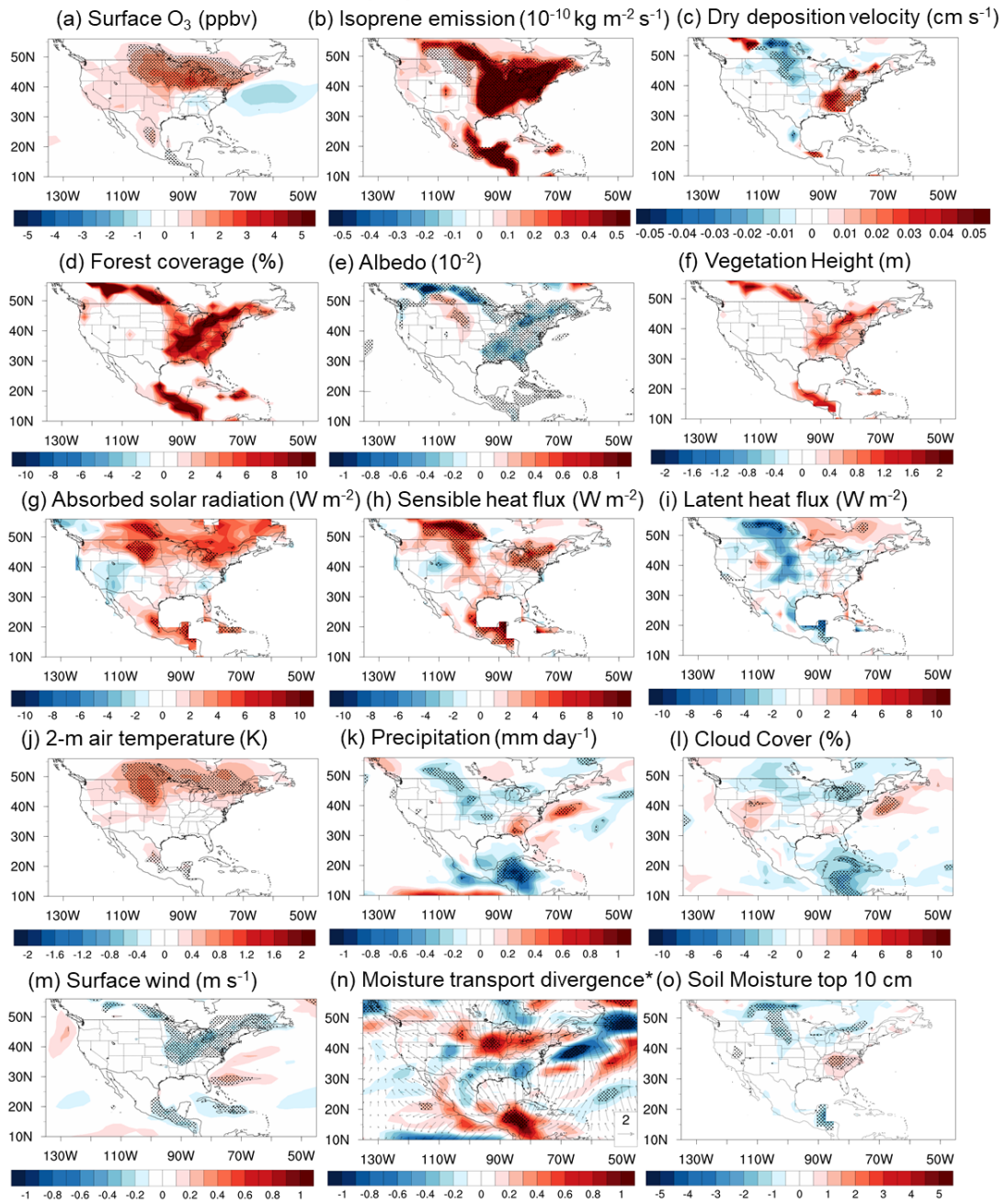
551 3.3.1 North America under RCP4.5 reforestation

552 For RCP4.5, North America is subjected to intensive regional changes in the
553 land cover over the eastern US and southern Canada (Fig. 5d). Significant changes in
554 surface ozone (Fig. 4a) and 2-m air temperature (Fig. 4d) are found over large
555 continuous areas in North America, including both the regions with intensive LULCC
556 and regions where LULCC is minimal. Let us first focus on the forested regions with
557 intensive LULCC (Fig. 5d), where reforestation results in a significant decrease in
558 surface albedo (Fig. 5e). In the boreal and temperate mixed forests of southern
559 Canada and northeastern US, such an albedo reduction results in a substantial
560 enhancement in absorbed solar radiation (Fig. 5g). Typical of these forest types, the
561 enhanced net radiation is in turn largely dissipated by higher sensible heat (Fig. 5h)
562 instead of latent heat (Fig. 5i), resulting in a 0.5–1 K rise in average air temperature
563 (Fig. 5j). This generates a warmer and drier boundary layer with suppressed
564 precipitation (Fig. 5k), cloud cover (Fig. 5l), and soil moisture (Fig. 5o), constituting a
565 feedback that likely further enhances net radiation. All these meteorological changes
566 contribute to higher surface ozone concentrations (Fig. 5a) beyond the

567 biogeochemical effects alone. In southern Canada, the drier conditions even help
568 suppress dry deposition (Fig. 5c), further enhancing ozone there. These
569 biogeophysical effects can be summarized by the cross-amplifying pathways in the
570 blue box in Fig. 1. Furthermore, reduced wind speed (Fig. 5m) following enhanced
571 roughness (as represented by vegetation height in Fig. 5f) may also reduce moisture
572 transport to these forests, inducing a greater moisture divergence there (Fig. 5n).

573 In contrast, in the subtropical broadleaf forests in the southeastern US,
574 enhanced forest cover and albedo instead lead to greater moisture convergence from
575 the Gulf of Mexico (Fig. 5n). This generates more favorable water conditions that not
576 only dampen meteorological changes there but also promote dry deposition, leading
577 to only slight changes in ozone. These can also be seen in the cross-counteracting
578 pathways in the blue box of Fig. 1.

RCP4.5 projected 2050 TIMESLC LULCC



579

580

Figure 5. Changes in surface ozone, isoprene emission, dry deposition velocity, projected forest,

581

simulated surface albedo, vegetation height, surface net solar radiation, sensible and latent heat fluxes,

582

2-m air temperature, precipitation, cloud cover, surface wind, vertically integrated moisture transport

583

divergence (vector: kg m⁻¹ s⁻¹, shading: 10⁻⁵ kg m⁻² s⁻¹), and soil moisture at top 10-cm layer during the

584

boreal summer over North America due to 2000-to-2050 RCP4.5 projected LULCC. Regions with dots

585

indicate changes that are significant at the 95% confidence level.

586

587 Surface ozone also increases significantly over the locations where land use
588 does not change significantly, especially over the Midwest and Great Plains regions of
589 north-central US (Figs. 5a and 5d). The ozone enhancement is found to correspond to
590 the drier, warmer and sunnier conditions there that can be considered as “remote
591 effects” of LULCC. Such conditions are associated with enhanced moisture
592 divergence (Fig. 5n), which could be caused by the stronger convergence over the
593 surrounding reforested regions that diverges moisture flow from the Great Plains, as
594 well as reduced surface wind speed (Fig. 5m) that can influence regional moisture
595 transport to these regions. The vertically integrated moisture fluxes at present-day
596 conditions are shown in Fig. S3a, illustrating that normally moisture transport from
597 the Gulf of Mexico is deflected by the Rocky Mountains and toward the eastern and
598 north-central US. Due to reforestation, moisture transport is deflected further east and
599 it generates an anomalous moisture flux divergence around the Midwest and Great
600 Plains, resulting in drier conditions in these regions. The drier and warmer boundary
601 layer are also reflected by the lower precipitation (Fig. 5k), cloud cover (Fig. 5l), soil
602 moisture (Fig. 5o), latent heat (Fig. 5i), and the associated higher net radiation (Fig.
603 5g), sensible heat (Fig. 5h) and air temperature (Fig. 5j). The lower soil moisture can
604 also reduce dry deposition there (Fig. 5c). All these changes can act together to
605 enhance surface ozone over the north-central US as remote effects of LULCC
606 elsewhere; these pathways can be summarized by the yellow box in Fig. 1.

607

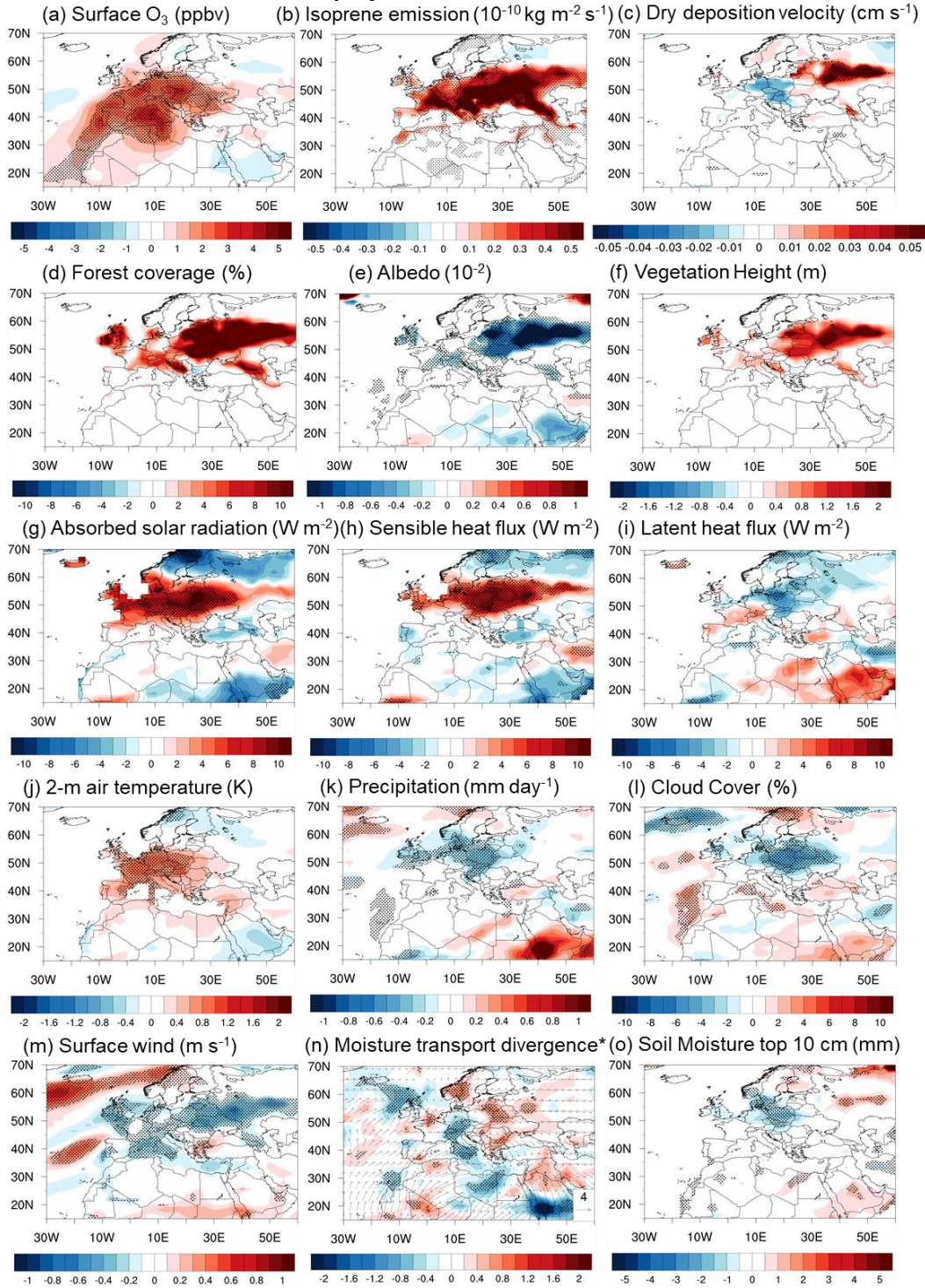
608 3.3.2 Europe under RCP4.5 reforestation

609 Substantial increases in surface ozone (Fig. 6a) and air temperature (Fig. 6j)
610 are found in Europe due to the RCP4.5 LULCC scenario, whereby substantial
611 reforestation occurs over in the boreal and temperate mixed forests in the European

612 continental regions (Fig. 6d), modifying surface energy balance significantly. Over
613 the regions with intensive LULCC, the biogeophysical pathways shaping boundary-
614 layer meteorology and ozone are largely similar to southern Canada and northeastern
615 US, where the forest types are similar (see blue box in Fig. 1). In brief, reduced
616 albedo (Fig. 6e) leads to enhanced net radiation (Fig. 6g) and sensible heat (Fig. 6h),
617 raising 2-m air temperature over a large area by 0.4–1.2 K (Fig. 6j), and constituting a
618 hydrometeorological feedback that reduces precipitation (Fig. 6k), cloud cover (Fig.
619 6l), and soil moisture (Fig. 6o). These changes generate warmer, drier and sunnier
620 conditions over the forests that favor higher ozone levels. Reforestation also decreases
621 surface wind speed (Fig. 6m) and moisture transport at the near-surface level.

622 The increases in surface ozone are also found to extend westward and
623 southward beyond the regions with intensive LULCC, likely reflecting remote effects
624 (Fig. 6a). The lower-level wind patterns at 850 hPa under present-day conditions are
625 shown in Fig. S3b, showing that reforested regions are originally on the southerly
626 branch (eastern part) of the Azores High anticyclone. Circulation changes in response
627 to reforestation appears to enable the anticyclonic system to extend eastward,
628 allowing sunny and warm conditions typical of the Azores High to prevail over much
629 of western Europe and parts of North Africa, and enhancing surface ozone there.

RCP4.5 projected 2050 TIMESLC LULCC



630

631 Figure 6. Similar to Fig. 5 but for Europe under RCP4.5.

632

633

Overall, we find that biogeophysical effects can have strong impacts on

634

surface ozone through modifying local and remote meteorological conditions such as

635

surface warming, drying and circulation anomalies initiated by local LULCC (Fig. 1).

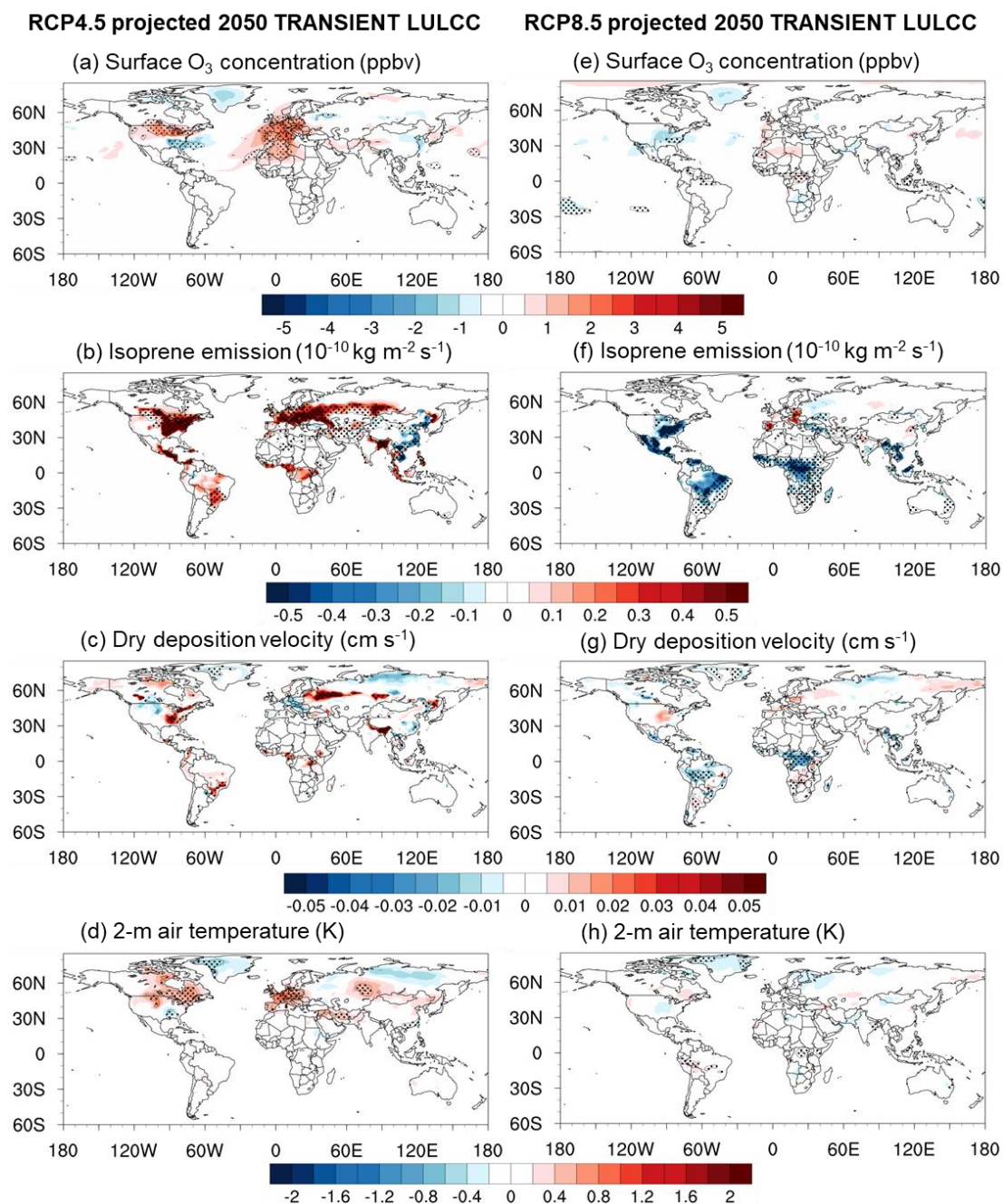
636 Our results of temperature changes are consistent with the previous study of Swann et
637 al. (2012) that illustrated the local and remote climate effects of the northern
638 midlatitude reforestation. They conducted a model experiment with extreme
639 afforestation, and found substantial warming in North America and Europe. In
640 addition, Govindasamy and Caldeira (2001) and Unger (2014) also found surface
641 cooling due to deforestation.

642

643 3.3.3 Transient experiments versus time-slice experiments

644 In the above sections, for a direct, parallel comparison with the Off-line
645 configurations, we have used the time-sliced experiments with the present-day land
646 cover in year 2000 and future land cover in year 2050. However, in reality the
647 LULCC is transient with the land cover changing gradually; therefore, transient runs
648 in On-line mode with the land cover evolving from the present-day all the way to year
649 2065 are also conducted (On-line_45 and On-line_85, each with two ensemble
650 members; see Table 1). Fig. 7 shows the changes in ozone and other variables from
651 the transient simulations, using 2036 to 2065 as the 30-year averaging period to
652 capture interannual variability. We find that changes in ozone, 2-m air temperature,
653 and other factors controlling ozone are very similar between the transient and time-
654 sliced runs (see also Table 2), with only statistically insignificant differences in
655 different variables in most places (see Fig. S6 in the supplement). The consistent
656 simulated results from the transient (Fig. 7) and time-sliced (Fig. 4) LULCC further
657 reflect the robustness of the LULCC-induced signals at least over North America and
658 Europe, which are strong enough to cause changes in meteorology and ozone
659 pollution in places remote from LULCC, and indicate that the atmospheric responses

660 and biogeophysical effects are generally fast-responding at a quasi-steady state on
 661 timescales of years to decades with respect to the slow LULCC.



662
 663 Figure 7. Similar to Fig. 4 but these results are from the transient simulations On-line_45 and On-
 664 line85 (Table 1), averaged over the two ensemble members for each scenario.
 665

666 **4. Conclusions and Discussion**

667 LULCC is expected to continue to co-occur with future socioeconomic
668 development and anthropogenic emission reduction strategies. These changes likely
669 had, and will continue to have a large impact on air quality and climate. However, the
670 impacts of LULCC on surface ozone pollution are not fully understood, and the
671 attribution to different LULCC-mediated pathways is far from complete. Here, we
672 investigate and quantify specifically the biogeochemical effects (via modifying
673 ozone-relevant chemical fluxes), biogeophysical effects (via modifying the overlying
674 meteorological environment), and the combined effects of LULCC on surface ozone
675 air quality.

676 We address the biogeochemical effects alone by performing CESM
677 simulations with prescribed meteorology, and investigate the combined effects using
678 atmosphere-chemistry-land coupled configuration with dynamic meteorology. We
679 find that the biogeochemical effects of changing isoprene emission and dry deposition
680 following LULCC mostly offset each other, resulting in only modest changes in
681 ozone by up to 2 ppbv from 2000 to 2050. However, surface ozone can be
682 significantly altered by up to 5 ppbv when considering the combined effects
683 associated with the LULCC. In particular, the biogeophysical effects facilitated
684 through temperature changes plays a critical role in shaping surface ozone. We find
685 that surface ozone changes correspond well with temperature changes in RCP4.5 over
686 both regions with intensive LULCC and regions with limited LULCC.

687 The surface ozone changes due to future LULCC are comparable with
688 anthropogenic emissions and climate, and thus should be taken into account in future
689 research and policy planning. For example, summertime surface ozone changes
690 induced by climate change alone are projected to increase by 1–10 ppb in the US,

691 Europe, East and South Asia (e.g., Jacob and Winner, 2009; Fiore et al., 2012). It is
692 also found that the combined effects of changing climate, emissions and land cover on
693 surface ozone are up to 10 ppb in the US under two RCP scenarios, and the
694 contributions from the three factors have comparable magnitudes although of
695 different signs (Val Martin, et al., 2015). Wang et al. (2011) found that in China,
696 summertime surface ozone decreases by ~10 ppb on average with a maximum
697 reduction of 25 ppb if all anthropogenic emissions are removed. Our simulated ozone
698 changes induced by LULCC are substantial and within the same order of magnitude
699 as the above studies and others that considered meteorological responses to LULCC
700 (Ganzeveld et al., 2010; Val Martin et al., 2015). This highlights the important roles
701 of LULCC in modulating surface ozone.

702 The mechanisms behind hydrometeorological responses to LULCC are
703 summarized in Fig. 1. In brief, first, surface properties and processes (e.g., surface
704 albedo and evapotranspiration) are altered, leading to changes in the surface energy
705 balance. In boreal and temperate mixed forests, the albedo effect dominates, leading
706 to higher net radiation, sensible heat and surface temperature, but reduced
707 precipitation, cloud cover and soil moisture. These local changes can also induce a
708 regional circulation response, in particular the formation of anomalous moisture
709 divergence and corresponding warmer and drier conditions over the surrounding
710 regions even with limited LULCC. In subtropical broadleaf forests, however, both the
711 albedo and evapotranspiration effects are important and they tend to offset each other,
712 leading to minimal hydrometeorological changes.

713 In our analysis of LULCC-induced hydrometeorological changes, we have
714 focused on the surface and the overlying boundary layer. Many studies have found
715 that LULCC-induced surface changes can propagate to upper levels as high as 200

716 hPa (e.g., Chase et al., 2000; Swann et al., 2012; Medvigy, et al., 2013; Xu et al.,
717 2015; Jia et al., 2019). In our study, significant meteorological changes can be
718 detected at the upper levels up to 200 hPa due to LULCC (not shown), which can lead
719 to circulation changes, storm track displacement, and anomalous subsidence
720 especially at midlatitudes, likely constituting feedbacks on precipitation, moisture
721 transport, and temperature. However, we find no clear conclusions as to whether these
722 upper-level changes and feedbacks could have sufficient influence on ozone-relevant
723 hydrometeorological conditions beyond that can be explained by boundary-layer
724 dynamics alone.

725 Weaker responses of temperature as well as of surface ozone to LULCC are
726 found in RCP8.5 compared with those in RCP4.5. The different extent of temperature
727 responses can be attributed to the location where LULCC occurs. For RCP4.5,
728 LULCC is most intense in the midlatitude regions of the Northern Hemisphere. In
729 contrast, most LULCC for RCP8.5 occurs over the equatorial regions and Southern
730 Hemisphere. Temperature responses to LULCC may be less sensitive to tropical
731 changes or changes over the Southern Hemisphere that is dominated by the vast
732 oceanic expanse. Van der Molen et al (2011) using other models also found similar
733 patterns, and named such climate responses to LULCC as “tropical damping”. The
734 classical theory of such “tropical damping” is associated with a decrease in cloud
735 cover after deforestation, which then results in increased incoming radiation at the
736 surface and a lower planetary albedo, both counteracting the increase in surface
737 albedo with deforestation.

738 Our study has several limitations. First, the energy transport between the
739 ocean and land has not been taken into account. Although using a fully interactive
740 ocean component would increase the variability of simulated climate and decrease the

741 signal-to-noise ratio in sensitivity experiments using small forcings, such as LULCC
742 (e.g., Davin and de Noblet-Ducoudre 2010, Brovkin et al., 2013), coupled
743 atmosphere-ocean simulations are crucial for future climate change projections for the
744 longer term (e.g., well past the end of the 21st century). In addition, future LULCC
745 projections in RCPs are predicted from the ensemble of socioeconomic and emission
746 scenarios to match identified pathways of greenhouse gas concentrations. Large
747 uncertainties remain in such projections, calling for more skillful design of LULCC-
748 related metrics and the corresponding spatial patterns for better air quality predictions.
749 Third, the biogeochemical effects of LULCC on ozone in this study do not consider
750 climatic changes or anthropogenic emission change, but only focus on the more
751 immediate effects generated from LULCC such as isoprene emission and dry
752 deposition, mostly due to model limitations. For example, NO_x emission is projected
753 to decline sharply over the northeastern US in RCP4.5. As NO_x level decreases, ozone
754 production may become more NO_x-limited and thus the sensitivity to isoprene
755 emission may be reduced, rendering the overall biogeochemical effects of LULCC
756 smaller. However, since the biogeophysical effects operate in locations remote from
757 the source regions, they may be less affected by NO_x emission changes in the source
758 regions. The full biogeochemical effects of LULCC on ozone that include
759 biogeochemical cycle-climate feedbacks and co-effects of anthropogenic emission
760 and LULCC will warrant further investigation but will foreseeably present greater
761 challenges for process attribution and interpretation.

762 Atmospheric internal variability is one factor that could affect the significance
763 of our results. Large internal variability of the climate system reduces the signal-to-
764 noise ratio for LULCC-induced climatic changes (Deser et al., 2012). To ascertain the
765 impacts of such variability, we have adopted an analysis period of 30 years for both

766 the time-sliced simulations (looping over the single-year LULCC forcing) and 2-
767 member ensemble transient LULCC simulations. Results from both simulation
768 approaches all show broadly consistent signals induced by LULCC in North America
769 and Europe, indicating the significance of our results and the strong signal-to-noise
770 ratios at least over those continents. When applicable, more ensemble members for
771 transient simulations can be used to further confirm the impacts of such variability.
772 Furthermore, we have compared the magnitudes of interannual standard deviations of
773 near-surface temperature of the CTL run with the LULCC-induced climate signals.
774 Our results show that the climate signals are not weak and can be regionally
775 comparable to interannual variability at midlatitudes (Fig. S4), e.g., over North
776 America and Europe. It is also noteworthy that the time-sliced experiments with
777 single-year forcing looped for multiple years give results very similar to the transient
778 simulations, further pointing to the robustness of LULCC impacts.

779 Our study highlights the complexity of land surface forcing and the
780 importance of biogeophysical effects of LULCC on surface ozone air quality,
781 emphasizing the importance of LULCC in shaping atmospheric chemistry that could
782 be as important as anthropogenic emissions and climate. Our study can provide
783 important reference for policy makers to consider the substantial roles of LULCC in
784 tackling air pollution and climate change, to develop a more comprehensive set of
785 climatically relevant metrics for the management of the terrestrial biosphere, as well
786 as to explore co-benefits among air pollution, climate change and land use
787 management strategies.

788

789

790

791 **Author Contribution**

792 L. Wang designed the model experiments, performed numerical simulations
793 and analysis, and co-wrote the manuscript; A. P. K. Tai and C.-Y. Tam are the co-
794 principal investigators, who designed the research, performed some of the analysis,
795 and co-wrote the manuscript; and all authors contributed to the interpretation of the
796 results and writing of the paper.

797

798 **Acknowledgments**

799 This work was supported by the Vice-Chancellor Discretionary Fund (Project
800 ID: 4930744) from The Chinese University of Hong Kong (CUHK) given to the
801 Institute of Environment, Energy and Sustainability. It is also supported by a General
802 Research Fund grant (Project ID: 14306015) from the Research Grants Council of
803 Hong Kong given to A. P. K. Tai.

804

805

806 **References**

- 807 Arora, V. K., and Montenegro, A.: Small benefits provided by realistic afforestation
808 efforts. *Nat. Geosci.*, 4, 514-518. <https://doi.org/10.1038/ngeo1182>, 2011.
- 809 Avnery S., Mauzerall D. L., Liu J., and Horowitz L. W.: Global crop yield reductions
810 due to surface ozone exposure: 2. Year 2030 potential crop production losses and
811 economic damage under two scenarios of O₃ pollution, *Atmos. Environ.*, 45, 2297-
812 2309, <https://doi.org/10.1016/j.atmosenv.2011.01.002>, 2011.
- 813 Betts, R. A.: Biogeophysical impacts of land use on present-day climate: near-surface
814 temperature change and radiative forcing, *Atmos. Sci. Lett.*, 2, 39-51,
815 <https://doi.org/10.1006/asle.2001.0023>, 2001.
- 816 Boisier, J. P., de Noblet-Ducoudré, N., Pitman, A. J., Cruz, F. T., Delire, C., van den
817 Hurk, B. J. J. M., . . . Voltaire, A.: Attributing the impacts of land-cover changes in
818 temperate regions on surface temperature and heat fluxes to specific causes: Results
819 from the first LUCID set of simulations. *Journal of Geophysical Research:*
820 *Atmospheres*, 117, D12. <https://doi.org/10.1029/2011JD017106>, 2012.
- 821 Bonan, G. B.: Forests and climate change: Forcings, feedbacks, and the climate
822 benefits of forests. *Science*, 320, 1444-1449, <https://doi.org/10.1126/science.1155121>,
823 2008.
- 824 Bonan, G.: Forests, Climate, and Public Policy: A 500-Year Interdisciplinary
825 Odyssey, *Annu. Rev. Ecol. Evol. Syst.*, 47, 97-121, <https://doi.org/10.1146/annurev-ecolsys-121415-032359>, 2016.
- 827 Brovkin, V., Boysen L., Arora, V. K., Boisier, J. P., Cadule, P., Chini, L., Claussen,
828 M., Friedlingstein, P., Gayler, V., van den Hurk, B. J. J. M., Hurtt, G. C., Jones, C. D.,
829 Kato, E., de Noblet-Ducoudré, N., Pacifico, F., Pongratz, J., and Weiss, M.: Effect of
830 anthropogenic land-use and land-cover changes on climate and land carbon storage in

831 CMIP5 projections for the twenty-first century, *J. Clim.*, 26, 6859-6881,
832 <https://doi.org/10.1175/JCLI-D-12-00623.1>, 2013.

833 Brown-Steiner, B., Hess, P. G., and Lin, M. Y.: On the capabilities and limitations of
834 GCM simulations of summertime regional air quality: A diagnostic analysis of
835 ozone and temperature simulations in the US using CESM CAM-Chem, *Atmospheric*
836 *Environment*, 101, 134-148, <https://doi.org/10.1016/j.atmosenv.2014.11.001>, 2015.

837 Chase, T., Pielke, R., Kittel, T., Nemani, R., and Running, S.: Simulated Impacts of
838 Historical Land Cover Changes on Global Climate in Northern Winter, *Clim.*
839 *Dynam.*, 16, 93-105, <https://doi.org/10.1007/s003820050007>, 2000 .

840 Cooper, O. R., Parrish, D. D., Stohl, A., Trainer, M., Nédélec, P., Thouret,
841 V., ...Avery, M. A.: Increasing springtime ozone mixing ratios in the free troposphere
842 over western North America, *Nature*, 463, 344-348, doi:10.1038/nature08708, 2010.

843 de Noblet-Ducoudré, N., Boisier, J. P., Pitman, A., Bonan, G. B., Brovkin, V., Cruz,
844 F., ...Voldoire, A.: Determining robust impacts of land-use-induced land cover
845 changes on surface climate over North America and Eurasia: Results from the first set
846 of LUCID experiments. *J. Clim.*, 25, 3261-3281. [https://doi.org/10.1175/JCLI-D-11-](https://doi.org/10.1175/JCLI-D-11-00338.1)
847 [00338.1](https://doi.org/10.1175/JCLI-D-11-00338.1), 2012.

848 Deser, C., Knutti, R., Solomon, S., Phillips, A.: Communication of the role of natural
849 variability in future North American Climate. *Nature Clim. Change*, 2, 775-779,
850 doi:10.1038/nclimate1562, 2012.

851 Devaraju, N., Bala, G., Modak, A.: Effects of large-scale deforestation on
852 precipitation in the monsoon regions: Remote versus local effects. *PNAS*, 112, 3257-
853 3262, doi:10.1073/pnas.1423439112, 2015.

854 Doherty, R. M., Wild, O., Shindell, D. T., Zeng, G., MacKenzie, I. A., Collins, W. J.,
855 Fiore, A. M., Stevenson, D. S., Dentener, F. J., Schultz M. G., Hess, P., Derwent, R.

856 G., and Keating, T. J.: Impacts of climate change on surface ozone and
857 intercontinental ozone pollution: A multi-model study, *J. Geophys. Res. Atmos.*, 118,
858 1-20, <https://doi.org/10.1002/jgrd.50266>, 2013.

859 Emmons, L. K., Walters, S., Hess, P. G., Lamarque, J.-F., Pfister, G. G., Fillmore, D.,
860 Granier, C., Guenther, A., Kinnison, D., Laepple, T., Orlando, J., Tie, X., Tyndall, G.,
861 Wiedinmyer, C., Baughcum, S. L., and Kloster, S.: Description and evaluation of the
862 Model for Ozone and Related chemical Tracers, version 4 (MOZART-4), *Geosci.*
863 *Model Dev.*, 3, 43-67, <https://doi.org/10.5194/gmd-3-43-2010>, 2010.

864 Fiore, A. M., Horowitz, L. W., Purves, D. W., Levy II, H., Evans, M. J., Wang, Y.,
865 Li, Q., and Yantosca, M.: Evaluating the contribution of changes in isoprene
866 emissions to surface ozone trends over the eastern United States, *J. Geophys. Res.*
867 *Atmos.*, 110, D12303, <https://doi.org/10.1029/2004JD005485>, 2005.

868 Fiore, A. M., Naik, V., Spracklen, D. V., Steiner, A., Unger, N., Prather, M., and
869 Bergmann, D.: Global air quality and climate, *Chem. Soc. Rev.*, 41, 6663-6683, DOI:
870 10.1039/C2CS35095E, 2012.

871 Fu, Y., and Tai, A. P. K.: Impact of climate and land cover changes on tropospheric
872 ozone air quality and public health in East Asia between 1980 and 2010, *Atmos.*
873 *Chem. Phys.*, 15, 10093-10106, <https://doi.org/10.5194/acp-15-10093-2015>, 2015.

874 Ganzeveld, L., Bouwman, L., Stehfest, E., van Vuuren, D. P., Eickhout, B., and
875 Lelieveld, J.: Impact of future land use and land cover changes on atmospheric
876 chemistry-climate interactions, *J. Geophys. Res. Atmos.*, 115, D23301,
877 <https://doi.org/10.1029/2010JD014041>, 2010.

878 Govindasamy, B., and Caldeira, K.: Land use changes and Northern Hemisphere
879 cooling, *Geophys. Res. Lett.*, 28, 291-294, <https://doi.org/10.1029/2000GL006121>,
880 2001.

881 Guenther, A. B., Jiang, X., Heald, C. L., Sakulyanontvittaya, T., Duhl, T., Emmons,
882 L. K., and Wang, X.: The Model of Emissions of Gases and Aerosols from Nature
883 version 2.1 (MEGAN2.1): an extended and updated framework for modeling biogenic
884 emissions, *Geosci. Model Dev.*, 5, 1471-1492, [https://doi.org/10.5194/gmd-5-1471-](https://doi.org/10.5194/gmd-5-1471-2012)
885 2012, 2012.

886 Henderson-Sellers, A., Dickinson, R. E., Durbidge, T. B., Kennedy, P. J., McGuffie,
887 K., and Pitman, A. J.: Tropical deforestation: Modeling local- to regional-scale
888 climate change, *J. Geophys. Res. Atmos.*, 98, 7289-7315,
889 <https://doi.org/10.1029/92JD02830>, 1993.

890 Heald C. L., Henze, D. K., Horowitz, L. W., Feddema, J., Lamarque, J. - F.,
891 Guenther, A., Hess, P. G., Vitt, F., Seinfeld, J. F., Goldstein, A. H., and Fung, I.:
892 Predicted change in global secondary organic aerosol concentrations in response to
893 future climate, emissions, and land use change, *J. Geophys. Res.*, 113, D05211,
894 [doi:10.1029/2007JD009092](https://doi.org/10.1029/2007JD009092), 2008.

895 Heald, C. L., and Spracklen, D. V.: Land use change impacts on air quality and
896 climate, *Chem. Rev.*, 115, 4476-4496, <https://doi.org/10.1021/cr500446g>, 2015.

897 Heald, C. L., and Geddes, J. A.: The impact of historical land use change from 1850
898 to 2000 on secondary particulate matter and ozone, *Atmos. Chem. Phys.*, 16, 14997-
899 15010, <https://doi.org/10.5194/acp-16-14997-2016>, 2016.

900 Hurtt, G. C., Chini, L. P., Frohling, S., Betts, R. A., Feddema, J., Fischer, G., Fisk, J.
901 P., Hibbard, K., Houghton, R. A., Janetos, A., Jones, C. D., Kindermann, G.,
902 Kinoshita, T., Goldewijk, K. K., Riahi, K., Shevliakova, E., Smith, S., Stehfest, E.,
903 Thomson, A., Thornton, P., van Vuuren, D. P., and Wang, Y. P.: Harmonization of
904 land-use scenarios for the period 1500–2100: 600 years of global gridded annual land-

905 use transitions, wood harvest, and resulting secondary lands, *Climatic Change*, 109,
906 117-161, DOI:10.1007/s10584-011-0153-2, 2011.

907 Jacob, D. J., and Winner, D. A.: Effect of climate change on air quality, *Atmos.*
908 *Environ.*, 43, 51-63, <https://doi.org/10.1016/j.atmosenv.2008.09.051>, 2009.

909 Jerrett, M., Burnett, R. T., Pope, C. A., Ito, K., Thurston, G., Krewski, D., Shi, Y.,
910 Calle, E., and Thun, M.: Long-Term Ozone Exposure and Mortality, *New Engl. J.*
911 *Med.*, 360, 1085-1095, DOI: 10.1056/NEJMoa0803894, 2009.

912 Jia, G., Shevliakova, E., Artaxo, P., de Noblet-Ducoudré, N., Houghton, R., House, J.,
913 Kitajima, K., Lennard, C., Popp, A., Sirin, A., Sukumar, R., and Verchot, L.: Land-
914 climate interactions. In: *Climate Change and Land: an IPCC special report on climate*
915 *change, desertification, land degradation, sustainable land management, food security,*
916 *and greenhouse gas fluxes in terrestrial ecosystems* [Shukla, P. R, Skea, J., Calvo
917 Buendia, E., Masson-Delmotte, V., Pörtner, H.-O., Roberts, D. C., Zhai, P., Slade, R.,
918 Connors, S., van Diemen, R., Ferrat, M., Haughey, E., Luz, S., Neogi, S., Pathak, M.,
919 Petzold, D, Portugal Pereira, J., Vyas, P., Huntley, E., Kissick, K., Belkacemi, M.,
920 Malley, J. (eds.)]. 2019. In press.

921 Jiang, X., Wiedinmyer, C., Chen, F., Yang, Z.-L., and Lo, J. C.-F.: Predicted impacts
922 of climate and land use change on surface ozone in the Houston, Texas, area, *J.*
923 *Geophys. Res.*, 113, D20312, <https://doi.org/10.1029/2008JD009820>, 2008.

924 Kang, D., Aneja, V. P., Mathur, R., and Ray, J. D.: Nonmethane hydrocarbons and
925 ozone in three rural southeast United States national parks: A model sensitivity
926 analysis and comparison to measurements, *J. Geophys. Res.*, 108, 4604,
927 <https://doi.org/10.1029/2002JD003054>, 2003.

928 Kubistin, D., Harder, H., Martinez, M., Rudolf, M., ... , and Lelieveld, J. Hydroxyl
929 radicals in the tropical troposphere over the Suriname rainforest: comparison of

930 measurements with the box model MECCA. *Atmos. Chem. Phys.*, 10, 9705-9728,
931 2010. doi:10.5194/acp-10-9705-2010.

932 Lamarque, J.-F., Bond, T. C., Eyring, V., Granier, C., Heil, A., Klimont, Z., Lee, D.,
933 Liou, S. C., Mieville, A., Owen, B., Schultz, M. G., Shindell, D., Smith, S. J.,
934 Stehfest, E., Van Aardenne, J., Cooper, O. R., Kainuma, M., Mahowald, N.,
935 McConnell, J. R., Naik, V., Riahi, K., and van Vuuren, D. P.: Historical (1850-2000)
936 gridded anthropogenic and biomass burning emissions of reactive gases and aerosols:
937 methodology and application, *Atmos. Chem. Phys.*, 10, 7017-7039,
938 <https://doi.org/10.5194/acp-10-7017-2010>, 2010.

939 Lamarque, J. F., Emmons, L. K., Hess, P. G., Kinnison, D. E., Tilmes, S., Vitt, F.,
940 Heald, C. L., Holland, E. A., Lauritzen, P. H., Neu, J., Orlando, J. J., Rasch, P. J., and
941 Tyndall, G. K.: CAM-chem: description and evaluation of interactive atmospheric
942 chemistry in the Community Earth System Model, *Geosci. Model Dev.*, 5, 369-411,
943 <https://doi.org/10.5194/gmd-5-369-2012>, 2012.

944 Laguë, M., and Swann, A. S.: Progressive midlatitude afforestation: Impacts on
945 clouds, global energy transport, and precipitation. *J. Clim.*, 29, 5561-5573,
946 <https://doi.org/10.1175/JCLI-D-15-0748.1>, 2016.

947 Laguë, M. M., Bonan, G. B., Swann, A. S.: Separating the impact of individual land
948 surface properties on the terrestrial surface energy budget in both the coupled and un-
949 coupled land-atmosphere system. *J. Clim. Preprint*. 2019.

950 Lapina, K., Henze, D. K., Milford, J. B., Huang, M., Lin, M., Fiore, A. M.,
951 Carmichael, G., Pfister, G. G., and Bowman, K.: Assessment of source contributions
952 to seasonal vegetative exposure to ozone in the US, *J. Geophys. Res. Atmos.*, 119,
953 324-340, <https://doi.org/10.1002/2013JD020905>, 2014.

954 Lathière, J., Hauglustaine, D. A., Friend A. D., de Noblet-Ducoudré, N., Viovy N.,
955 and Folberth, G. A.: Impact of climate variability and land use changes on global
956 biogenic volatile organic compound emissions, *Atmos. Chem. Phys.*, 6, 2129-2146,
957 <https://doi.org/10.5194/acp-6-2129-2006>, 2006.

958 Lawrence, D. M., Oleson, K. W., Flanner, M. G., Thornton, P. E., Swenson, S. C.,
959 Lawrence, P. J., Zeng, X., Yang, Z.-L., Levis, S., Sakaguchi, K., Bonan, G. B., and
960 Slater, A. G.: Parameterization Improvements and Functional and Structural
961 Advances in Version 4 of the Community Land Model, *J. Adv. Model. Earth Syst.*, 3,
962 M03001, <https://doi.org/10.1029/2011MS00045>, 2011.

963 Lawrence, P. J., Feddema, J. J., Bonan, G. B., Meehl, G. A., O'Neill, B. C., Levis, S.,
964 Lawrence, D. M., Oleson, K. W., Kluzek, E., Lindsay, K., and Thornton, P. E.:
965 Simulating the Biogeochemical and Biogeophysical Impacts of Transient Land Cover
966 Change and Wood Harvest in the Community Climate System Model (CCSM4) from
967 1850 to 2100, *J. Climate.*, 25, 3071-3095, <https://doi.org/10.1175/JCLI-D-11-00256.1>,
968 2012.

969 Lau, N.-C.: Variability of the observed midlatitude storm tracks in relation to low-
970 frequency change in the circulation pattern, *J. Atmos. Sci.*, 45, 2718-2743,
971 [https://doi.org/10.1175/1520-0469\(1988\)045<2718:VOTOMS>2.0.CO;2](https://doi.org/10.1175/1520-0469(1988)045<2718:VOTOMS>2.0.CO;2), 1988.

972 Lin, M., Horowitz, L. W., Payton, R., Fiore, A. M., and Tonnesen G.: US surface
973 ozone trends and extremes from 1980 to 2014: quantifying the roles of rising Asian
974 emissions, domestic controls, wildfires, and climate, *Atmos. Chem. Phys.*, 17, 2943-
975 2970, <https://doi.org/10.5194/acp-17-2943-2017>, 2017.

976 Lin, M., Malyshev, S., Shevliakova, E., and co-authors. Sensitivity of ozone dry
977 deposition to ecosystem-atmosphere interactions: A critical appraisal of observations

978 and simulations, *Global Biogeochemical Cycles*, 33, 1264-1288,
979 <https://doi.org/10.1029/2018GB006157>, 2019.

980 Lee, X., Goulden, M. L., Hollinger, D. Y., Barr, A., Black, T. A., Bohrer, G., ...Zhao,
981 L. Observed increase in local cooling effect of deforestation at higher latitudes.
982 *Nature*, 479, 384-387. <https://doi.org/10.1038/nature10588>, 2011.

983 Malley, C. S., Henze, D. K., Kuylenstierna, J. C. I., Vallack, H. W., Davila, Y.,
984 Anenberg, S. C., Turner, M. C., and Ashmore, M. R.: Updated global estimates of
985 respiratory mortality in adults ≥ 30 years of age attributable to long-term ozone
986 exposure, *Environ, Health Perspect.*, 125, 087021, doi: 10.1289/EHP1390, 2017.

987 Matthews, H.D.D., Weaver, A.J.J., Meissner, K.J.J., Gillett, N.P.P. and Eby, M.:
988 Natural and anthropogenic climate change: incorporating historical land cover
989 change, vegetation dynamics and the global carbon cycle. *Clim. Dyn.*, 22, 461-479,
990 doi:10.1007/s00382-004-0392-2, 2004.

991 Medvigy, D., Walko, R., Otte, M., and Avissar, R. Simulated Changes in Northwest
992 U.S. Climate in Response to Amazon Deforestation. *J. Climate*, 26, 9115-9136,
993 <https://doi.org/10.1175/JCLI-D-12-00775.1>, 2013.

994 Myhre, G., et al.: Anthropogenic and Natural Radiative Forcing. In: *Climate Change*
995 2013: The Physical Science Basis. Contribution of Working Group I to the Fifth
996 Assessment Report of the Intergovernmental Panel on Climate Change (Stocker, T.F.,
997 et al., (eds.)). Cambridge University Press, Cambridge, United Kingdom and New
998 York, NY, USA, 2013.

999 Oleson, K. W., Lawrence D. W., and Bonan, G. B.: Technical description of version
1000 4.5 of the Community Land Model (CLM). NCAR Technical Note NCAR/TN-
1001 503+STR, National Centre for Atmospheric Research, Boulder, USA, 2013.

1002 Parrish, D. D., Lamarque, J. F., Naik, V., Horowitz, L., Shin-
dell, D. T., Staehelin, J.,
1003 Derwent, R., Cooper, O. R., Tanimoto, H., Volz-Thomas, A., and Gilge, S.: Long-
1004 term changes in lower tropospheric baseline ozone concentrations: Comparing
1005 chemistry-climate models and observations at northern midlatitudes, *J. Geophys. Res.*
1006 *Atmos.*, 119, 5719-5736, <https://doi.org/10.1002/2013JD021435>, 2014.

1007 Pfister, G. G., Emmons, L. K., Hess, P. G., Lamarque, J.-F., Orlando, J. J., Walters,
1008 S., Guenther, A., Palmer, P. I., and Lawrence, P. J.: Contribution of isoprene to
1009 chemical budgets: A model tracer study with the NCAR CTM MOZART-4, *J.*
1010 *Geophys. Res.*, 113, D05308, <https://doi.org/10.1029/2007JD008948>, 2008.

1011 Pitman, A. J., de Noblet-Ducoudre, N., Cruz, F. T., Davin, E. L., Bonan, G. B.,
1012 Brovkin, V., Claussen, M., Delire, C., Ganzeveld, L., Gayler, V., van den Hurk, B.,
1013 Lawrence, P. J., van der Molen, M. K., Muller, C., Reick, C. H., Seneviratne, S. I.,
1014 Strengers, B. J., and Voldoire, A.: Uncertainties in climate responses to past land
1015 cover change: First results from the LUCID intercomparison study, *Geophys. Res.*
1016 *Lett.*, 36, L14814, <https://doi.org/10.1029/2009GL039076>, 2009.

1017 Pongratz, J., Reick, C.H., Raddatz, T. and Claussen, M.: Biogeophysical versus
1018 biogeochemical climate response to historical anthropogenic land cover change.
1019 *Geophys. Res. Lett.*, 37, 1–5, doi:10.1029/2010GL043010, 2010.

1020 Porter, W. C., Heald, C. L., Cooley, D., and Russell, B.: Investigating the observed
1021 sensitivities of air-quality extremes to meteorological drivers via quantile regression,
1022 *Atmos. Chem. Phys.*, 15, 10349-10366, <https://doi.org/10.5194/acp-15-10349-2015>,
1023 2015.

1024 Pusede, S. E., Steiner, A. L., and Cohen, R. C.: Temperature and recent trends in the
1025 chemistry of continental surface ozone, *Chem. Rev.*, 115, 3898-3918,
1026 <https://doi.org/10.1021/cr5006815>, 2015.

1027 Rayner, N. A., Parker, D. E., Horton, E. B., Folland, C. K., Alexander, L. V., Rowell,
1028 D. P., Kent, E. C., and Kaplan, A.: Global analyses of sea surface temperature, sea
1029 ice, and night marine air temperature since the late nineteenth century, *J. Geophys.*
1030 *Res. Atmos.*, 108, D002670, <https://doi.org/10.1029/2002JD002670>, 2003.

1031 Riahi, K., Grübler, A., and Nakicenovic, N.: Scenarios of long-term socio-economic
1032 and environmental development under climate stabilization, *Technol. Forecast. Soc.*
1033 *Change*, 74, 887-935, <https://doi.org/10.1016/j.techfore.2006.05.026>, 2007.

1034 Riahi, K., Krey, V., Rao, S., Chirkov, V., Fischer, G., Kolp, P., Kindermann, G.,
1035 Nakicenovic, N., and Rafai, P.: RCP8.5-exploring the consequence of high emission
1036 trajectories, *Climatic Change*, 109:33, <https://doi.org/10.1007/s10584-011-0149-y>,
1037 2011.

1038 Ramankutty, N., Evan, A. T., Monfreda, C., and Foley, J. A.: Farming the planet: 1.
1039 Geographic distribution of global agricultural lands in the year 2000, *Glob.*
1040 *Biogeochem. Cyc.*, 22, GB1003, <https://doi.org/10.1029/2007GB002952>, 2008.

1041 Sadiq, M., Tai, A. P. K., Lombardozzi, D., and Val Martin, M.: Effects of ozone-
1042 vegetation coupling on surface ozone air quality via biogeochemical and
1043 meteorological feedbacks, *Atmos. Chem. Phys.* 17, 3055-3066,
1044 <https://doi.org/10.5194/acp-17-3055-2017>, 2017.

1045 Schnell, J. L., Prather, M. J., Josse, B., Naik, V., Horowitz, L. W., Zeng, G., Shindell,
1046 D. T., and Faluvegi, G.: Effect of climate change on surface ozone over North
1047 America, Europe, and East Asia, *Geophys. Res. Lett.*, 43, 3509-3518,
1048 <https://doi.org/10.1002/2016GL068060>, 2016.

1049 Shevliakova, E., Stouffer, R. J., Malyshev, S., Krasting, J. P., Hurtt, G. C., and Pacala,
1050 S. W. : Historical warming reduced due to enhanced land carbon uptake. *Proc. Natl.*
1051 *Acad. Sci.*, 110, 16730–16735, doi:10.1073/pnas.1314047110, 2013

1052 Simmons, C.T. and Matthews, H.D.: Assessing the implications of human land-use
1053 change for the transient climate response to cumulative carbon emissions. *Environ.*
1054 *Res. Lett.*, 11, doi:10.1088/1748-9326/11/3/035001, 2016.

1055 Squire, O. J., Archibald, A. T., Abraham, N. L., Beerling, D. J., Hewitt, C. N.,
1056 Lathière, J., Pike, R. C., Telford, P. J., and Pyle, J. A.: Influence of future climate and
1057 cropland expansion on isoprene emissions and tropospheric ozone, *Atmos. Chem.*
1058 *Phys.*, 14, 1011-1024, <https://doi.org/10.5194/acp-14-1011-2014>, 2014.

1059 Shen, L., Mickley, L. J., and Gilleland, E.: Impact of increasing heat waves on US
1060 ozone episodes in the 2050s: Results from a multimodel analysis using extreme value
1061 theory, *Geophys. Res. Lett.*, 43, 4017-4025, <https://doi.org/10.1002/2016GL068432>,
1062 2016.

1063 Swann, A. L. S., Fung, I. Y., and Chiang, J. C. H.: Mid-latitude afforestation shifts
1064 general circulation and tropical precipitation, *Proc. Natl. Acad. Sci., USA*, 109, 712-
1065 716, <https://doi.org/10.1073/pnas.1116706108>, 2012.

1066 Tai, A. P. K., Mickley, L. J., Heald, C. L., and Wu, S.: Effect of CO₂ inhibition on
1067 biogenic isoprene emission: Implications for air quality under 2000 to 2050 changes
1068 in climate, vegetation, and land use, *Geophys. Res. Lett.*, 40, 3479-3483,
1069 <https://doi.org/10.1002/grl.50650>, 2013.

1070 Tai, A. P. K., Val Martin, M. and Heald, C. L.: Threat to Future Global Food Security
1071 from Climate Change and Ozone Air Pollution, *Nat. Clim. Change*, 4, 817-821,
1072 <https://doi.org/10.1038/nclimate2317>, 2014.

1073 Tai, A. P. K., and Val Martin, M.: Impacts of ozone air pollution and temperature
1074 extremes on crop yields: Spatial variability, adaptation and implications for future
1075 food security, *Atmos. Environ.*, 169, 11-21, DOI10.1016/j.atmosenv.2017.09.002,
1076 2017.

1077 Taylor, K. E., Stouffer, R. J., and Meehl, G. A.: An overview of CMIP5 and the
1078 experiment design, *Bull. Am. Meteorol. Soc.*, 93, 485-498,
1079 <https://doi.org/10.1175/BAMS-D-11-00094.1>, 2012.

1080 Thomson, A. M., Calvin, K. V., Smith, S. J., Kyle, G. P., Volke, A., Patel, P.,
1081 Delgado-Arias, S., and Bond-Lamberty, B.: RCP4.5: a pathway for stabilization of
1082 radiative forcing by 2100, *Climatic Change*, 109, 77-94,
1083 <https://doi.org/10.1007/s10584-011-0151-4>, 2011.

1084 Thornton, J. A., Wooldridge, P. J., Cohen, R. C., Martinez, M., Harder, H., Brune, W.
1085 H., Williams, E. J., Roberts, J. M., Fehsenfeld, F. C., Hall, S. R., Shetter, R. E., Wert,
1086 B. P., and Fried, A.: Ozone production rates as a function of NO_x abundances and
1087 HO_x production rates in the Nashville urban plume, *J. Geophys. Res.*, 107,
1088 4146(D12), 4146, doi:10.1029/2001JD000932, 2002.

1089 Tian, H., Ren, W., Tao, B., Sun, G., Chappelka, A., Wang, X., Pan, S., Yang, J., Liu,
1090 J., Felzer, B., Melillo, J., and Reilly, J.: Climate extremes and ozone pollution: a
1091 growing threat to China's food security, *Ecosystem Health and Sustainability*, 2,
1092 e01203, <https://doi.org/10.1002/ehs2.1203>, 2016.

1093 Tilmes, S.: GEOS5 Global Atmosphere Forcing Data. Research Data Archive at the
1094 National Center for Atmospheric Research, Computational and Information Systems
1095 Laboratory, <http://rda.ucar.edu/datasets/ds313.0/>, 2016.

1096 Unger, N.: Human land-use-driven reduction of forest volatiles cools global climate,
1097 *Nat. Clim. Change*, 4, 907-910, <https://doi.org/10.1038/nclimate2347>, 2014.

1098 Val Martin, M., Heald, C. L., and Arnold, S. R.: Coupling dry deposition to
1099 vegetation phenology in the Community Earth System Model: Implications for the
1100 simulation of surface O₃, *Geophys. Res. Lett.*, 41, 2988-2996,
1101 <https://doi.org/10.1002/2014GL059651>, 2014.

1102 Val Martin, M., Heald, C. L., Lamarque, J.-F., Tilmes, S., Emmons, L. K., and
1103 Schichtel, B. A.: How emissions, climate, and land use change will impact mid-century
1104 air quality over the United States: a focus on effects at national parks, *Atmos. Chem.*
1105 *Phys.*, 15, 2805-2823, <https://doi.org/10.5194/acp-15-2805-2015>, 2015.

1106 van der Molen, M. K., van den Hurk, B. J. J. M., and Hazeleger, W.: A dampened
1107 land use change climate response towards the tropics, *Clim. Dyn.*, 37, 2035-2043,
1108 <https://doi.org/10.1007/s00382-011-1018-0>, 2011.

1109 van Vuuren, D. P., den Elzen, M. G. J., Lucas, P. L., Eickhout, B., Strengers, B. J.,
1110 van Ruijven, B., Wonink, S., and van Houdt, R.: Stabilizing greenhouse gas
1111 concentrations at low levels: an assessment of reduction strategies and costs, *Climatic*
1112 *Change*, 81, 119-159, <https://doi.org/10.1007/s10584-006-9172-9>, 2007.

1113 van Vuuren, D. P., Edmonds, J., Kainuma, M., Riahi, K., Thomson, A., Hibbard, K.,
1114 Hurtt, G. C., Kram, T., Krey, V., Lamarque, J. F., Masui, T., Meinshausen, M.,
1115 Nakicenovic, N., Smith, S. J., and Rose, S. K.: The representative concentration
1116 pathways: an overview, *Climatic Change*, 109, 5-31, [https://doi.org/10.1007/s10584-](https://doi.org/10.1007/s10584-011-0148-z)
1117 [011-0148-z](https://doi.org/10.1007/s10584-011-0148-z), 2011.

1118 Verbeke, T., Lathière, J., Szopa, S., and de Noblet-Ducoudré, N.: Impact of future
1119 land-cover changes on HNO₃ and O₃ surface dry deposition, *Atmos. Chem. Phys.*, 15,
1120 13555-13568, <https://doi.org/10.5194/acp-15-13555-2015>, 2015.

1121 von Kuhlmann, R., Lawrence, M. G., Poschl, U., and Crutzen, P. J.: Sensitivities in
1122 global scale modeling of isoprene, *Atmos. Chem. Phys.*, 4, 1-17,
1123 <https://doi.org/10.5194/acp-4-1-2004>, 2004.

1124 Wang, Y., Zhang, Y., Hao, J., and Luo, M.: Seasonal and spatial variability of surface
1125 ozone over China: contributions from background and domestic pollution, *Atmos.*
1126 *Chem. Phys.*, 11, 3511-3525, <https://doi.org/10.5194/acp-11-3511-2011>, 2011.

1127 Wang, Y., Shen, L., Wu, S., Mickley, L., He, J., and Hao, J.: Sensitivity of surface
1128 ozone over China to 2000-2050 global changes of climate and emissions, *Atmos.*
1129 *Environ.*, 75, 374-382, <https://doi.org/10.1016/j.atmosenv.2013.04.045>, 2013.

1130 Wesely, M.: Parameterization of surface resistances to gaseous dry deposition in
1131 regional-scale numerical models, *Atmos. Environ.*, 23, 1293-1304,
1132 [https://doi.org/10.1016/0004-6981\(89\)90153-4](https://doi.org/10.1016/0004-6981(89)90153-4), 1989.

1133 Wise, M., Calvin, K., Thomson, A., Clarke, L., Bond-Lamberty, B., Sands, R., Smith,
1134 S., J., Janetos, A., and Edmonds, J.: Implication of limiting CO₂ concentrations for
1135 land use and energy, *Science*, 324, 1183-1186, DOI: 10.1126/science.1168475,
1136 2009a.

1137 Wise, M., Calvin, K., Thomson, A., Clarke, L., Sands, R., Smith, S. J., Janetos, A.,
1138 and Edmonds, J.: The Implications of Limiting CO₂ Concentrations for Agriculture,
1139 Land-use Change Emissions, and Bioenergy, Technical Report, DOE Pacific
1140 Northwest National Laboratory, 2009b.

1141 Wong, A. Y. H., Tai, A. P. K., and Ip, Y.-Y.: Attribution and statistical
1142 parameterization of the sensitivity of surface ozone to changes in leaf area index
1143 based on a chemical transport model, *J. Geophys. Res. Atmos.*, 123, 1883-1898,
1144 <https://doi.org/10.1002/2017JD027311>, 2018.

1145 World Health Organization: WHO Air quality guidelines for particulate matter,
1146 ozone, nitrogen dioxide and sulfur dioxide, Global update 2005, Summary of risk
1147 assessment, 2005.
1148 (http://apps.who.int/iris/bitstream/10665/69477/1/WHO_SDE_PHE_OEH_06.02_eng
1149 .pdf).

1150 Wu, S., Mickley, L. J., Kaplan, J. O., and Jacob, D. J.: Impacts of changes in land use
1151 and land cover on atmospheric chemistry and air quality over the 21st century, *Atmos.*
1152 *Chem. Phys.*, 12, 1597-1609, <https://doi.org/10.5194/acp-12-1597-2012>, 2012.

1153 Xu, Z., Mahmood, R., Yang, Z.-L., Fu, C., and Su, H. Investigating diurnal and
1154 seasonal climatic response to land use and land cover change over monsoon Asia with
1155 the Community Earth System Model. *J. Geophys. Res. Atmos.*, 120, 1137-1152.
1156 <https://doi.org/10.1002/2014JD022479>, 2015.

1157 Xue, L., Wang, T., Louie, P. K. K., Luk, C. W. Y., Blake, D. R., and Xu, Z.:
1158 Increasing external effects negate local efforts to control ozone air pollution: A case
1159 study of Hong Kong and implications for other Chinese cities, *Environ. Sci. Technol.*,
1160 48, 10769-10775, <https://doi.org/10.1021/es503278g>, 2014.

1161 Yienger, J. J., and Levy II H.: Empirical model of global soil-biogenic NO_x
1162 emissions, *J. Geophys. Res. Atmos.*, 100, 11447-11464,
1163 <https://doi.org/10.1029/95JD00370>, 1995.

1164 Yue, X. and Unger, N.: Ozone vegetation damage effects on gross primary
1165 productivity in the United States, *Atmos. Chem. Phys.*, 14, 9137-9153,
1166 <https://doi.org/10.5194/acp-14-9137-2014>, 2014.

1167 Zhang, Q., Yuan, B., Shao, M., Wang, X., Lu, S., Lu, K., Wang, M., Chen, L., Chang,
1168 C.-C., and Liu, S. C.: Variations of ground-level O₃ and its precursors in Beijing in
1169 summertime between 2005 and 2011, *Atmos. Chem. Phys.*, 14, 6089-6101,
1170 <https://doi.org/10.5194/acp-14-6089-2014>, 2014.

1171 Zhou, D., Ding, A., Mao, H., Fu, C., Wang, T., Chan, L. Y., Ding, K., Zhang, Y., Liu,
1172 J., Lu, A., Hao, N.: Impacts of the East Asian monsoon on lower tropospheric ozone
1173 over coastal South China, *Environ. Res. Lett.*, 8, 044011, doi:10.1088/1748-
1174 9326/8/4/044011, 2013.

